Laser cooling of anions for ultracold antihydrogen

Alban Kellerbauer
Max Planck Institute for Nuclear Physics, Heidelberg

Max Planck Institute for Nuclear Physics

European Research Council

AEGIS experiment

- AEGIS: Antimatter Experiment: Gravity, Interferometry, Spectroscopy
- Main goal: Measurement of *g* with 1% precision on antihydrogen
- Requirements / challenges:
  - Production of a **bunched cold beam of antihydrogen** (100 mK)
  - Measurement of vertical beam deflection (10 µm drop over 1 m)

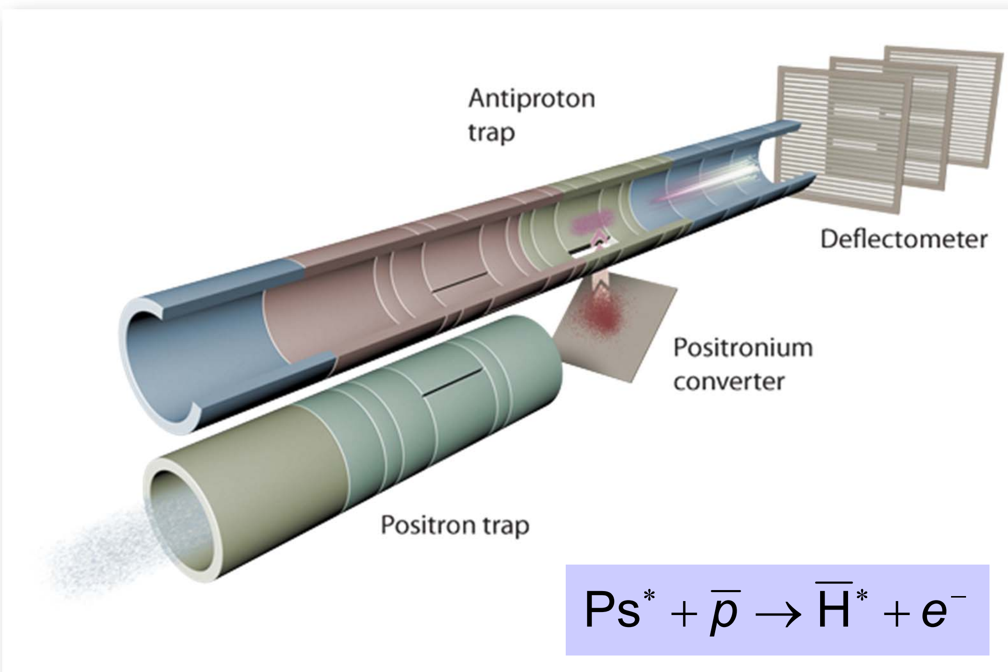

$$\mathrm{Ps}^* + \bar{p} \rightarrow \overline{\mathrm{H}}^* + e^-$$

[A.K. *et al.* (AEGIS Collaboration), Nucl. Instrum. Methods B **266** (2008) 351]

AEGIS experiment

- AEGIS: Antimatter Experiment: Gravity, Interferometry, Spectroscopy
- Main goal: Measurement of *g* with 1% precision on antihydrogen
- Requirements / challenges:
  - Production of a **bunched cold beam of antihydrogen** (100 mK)
  - Measurement of vertical beam deflection (10 µm drop over 1 m)

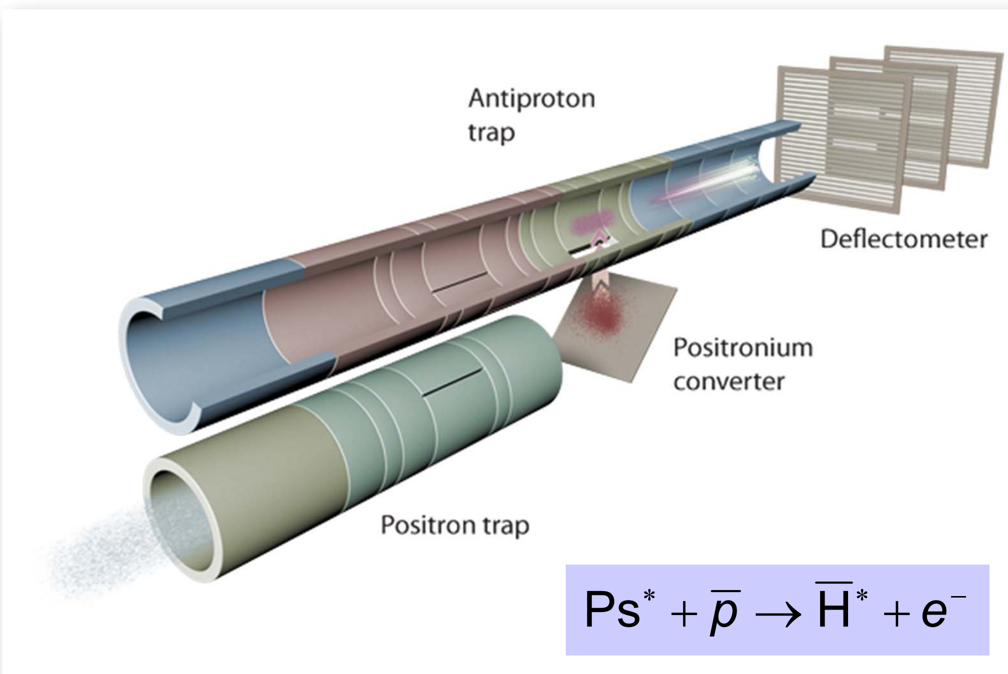

$$\mathrm{Ps}^* + \bar{p} \rightarrow \bar{\mathrm{H}}^* + e^-$$

[A.K. *et al.* (AEGIS Collaboration),
Nucl. Instrum. Methods B **266** (2008) 351]

Towards ultracold antihydrogen

- Proposed techniques:

1

Direct laser cooling of $\bar{H}$

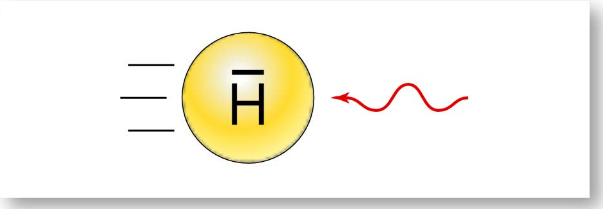

- requires cw Lyman-α laser for lowest temperatures
- doesn't increase $\bar{H}$ yield or trapped fraction

[P. H. Donnan *et al.* (ALPHA Collaboration), J. Phys. B **46** (2013) 025302]

Towards ultracold antihydrogen

- Proposed techniques:

1

Direct laser cooling of $\bar{H}$

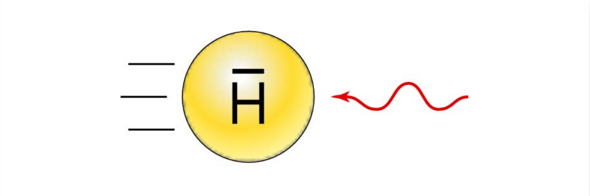

– requires cw Lyman-α laser for lowest temperatures

– doesn't increase $\bar{H}$ yield or trapped fraction

[P. H. Donnan *et al.* (ALPHA Collaboration), J. Phys. B **46** (2013) 025302]

2

Sympathetic cooling of $\bar{H}^+$ by laser-cooled cations

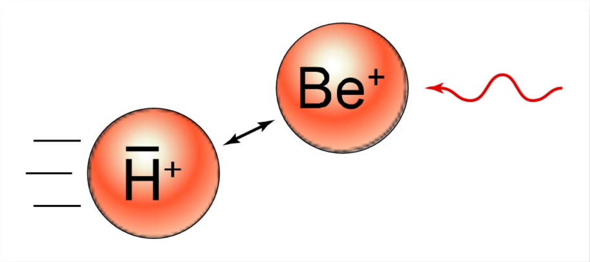

– low yield of $\bar{H}^+$

– complicated scheme

[L. Hilico *et al.* (GBAR Collaboration), Int. J. Mod. Phys. C. S. **30** (2014) 1460269]

Towards ultracold antihydrogen

- Proposed techniques:

1

Direct laser cooling of $\bar{\mathrm{H}}$

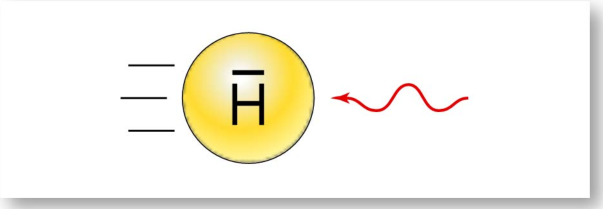

- requires cw Lyman-α laser for lowest temperatures
- doesn't increase $\bar{\mathrm{H}}$ yield or trapped fraction

[P. H. Donnan *et al.* (ALPHA Collaboration), J. Phys. B **46** (2013) 025302]

2

Sympathetic cooling of $\bar{\mathrm{H}}^+$ by laser-cooled cations

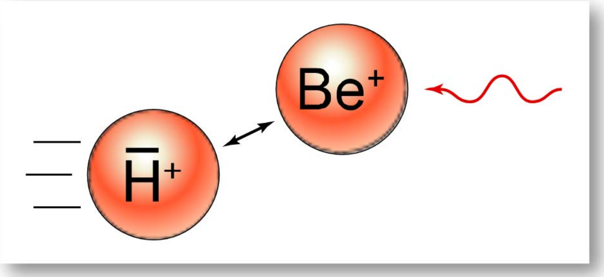

- low yield of $\bar{\mathrm{H}}^+$
- complicated scheme

[L. Hilico *et al.* (GBAR Collaboration), Int. J. Mod. Phys. C. S. **30** (2014) 1460269]

3

Sympathetic cooling of $\bar{p}$ by laser-cooled anions

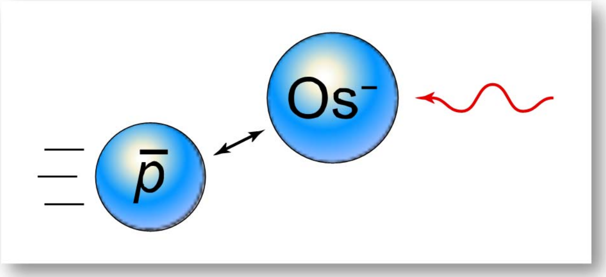

- laser cooling of anions has never been achieved

[A. K. & J. Walz, New J. Phys. **8** (2006) 1460269]

Laser cooling of atoms and ions

- Game-changing technique in many areas of AMO physics

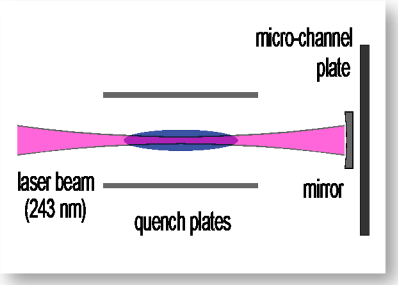

Atomic spectroscopy

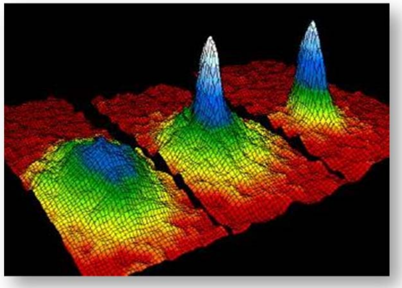

Bose–Einstein condensation

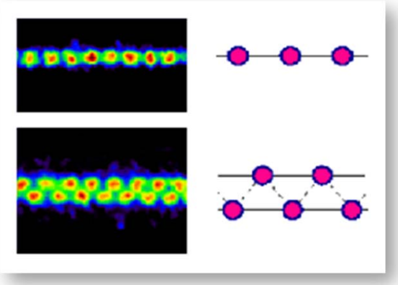

Coulomb crystals

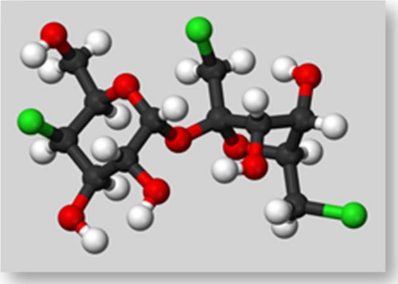

Molecular ions

Atomic clocks

- Laser cooling is an established technology
  - Positive ions 1978 (Toschek/Wineland)
  - Neutral atoms 1985 (Chu)
  - Negative ions **???**

Anion formation and binding

- Binding in atomic systems:

Coulomb potential	$\propto r^{-1}$
Polarization	$\propto r^{-4}$
Penetration	$\propto e^{-r}$

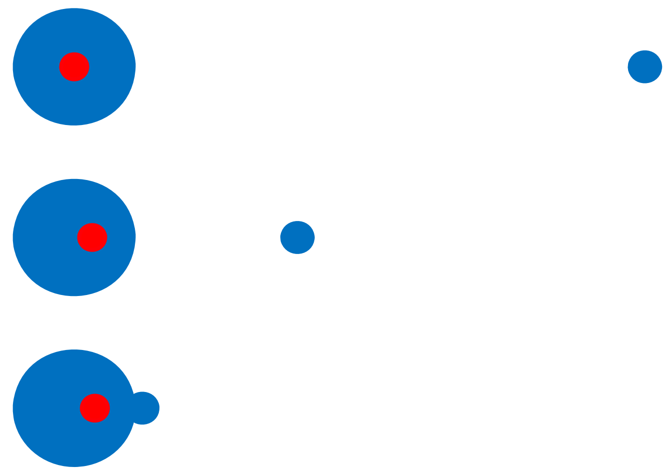

Anion formation and binding

- Binding in atomic systems:

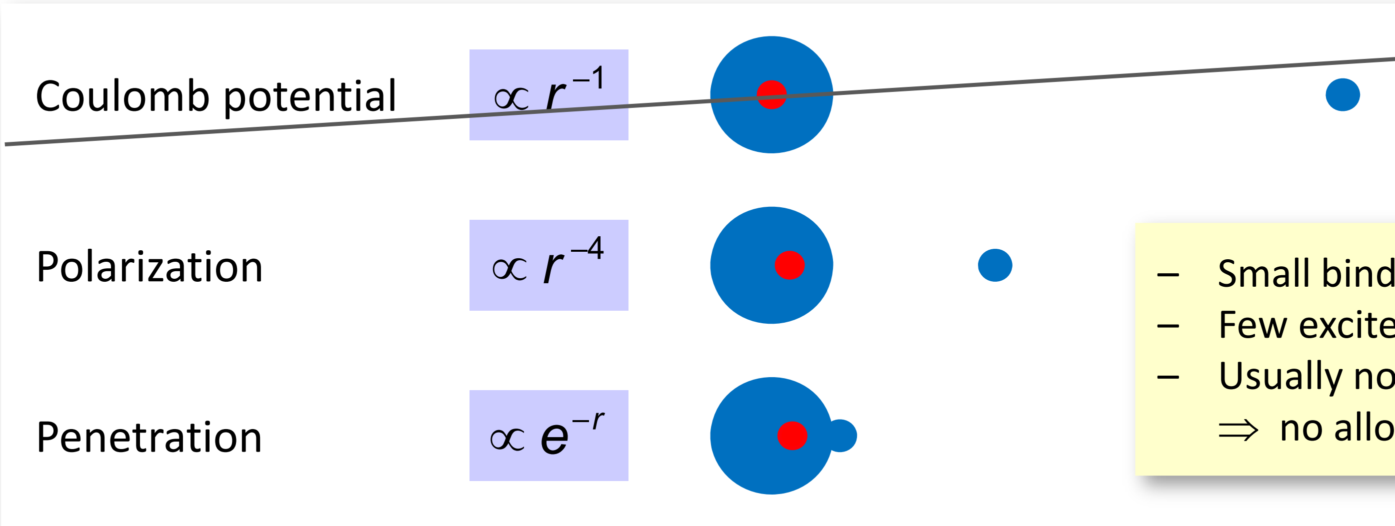

suppressed in atomic anions

- Small binding energy
- Few excited states
- Usually no states with opposite parity
  $\Rightarrow$ no allowed transitions

Anion formation and binding

- Binding in atomic systems:

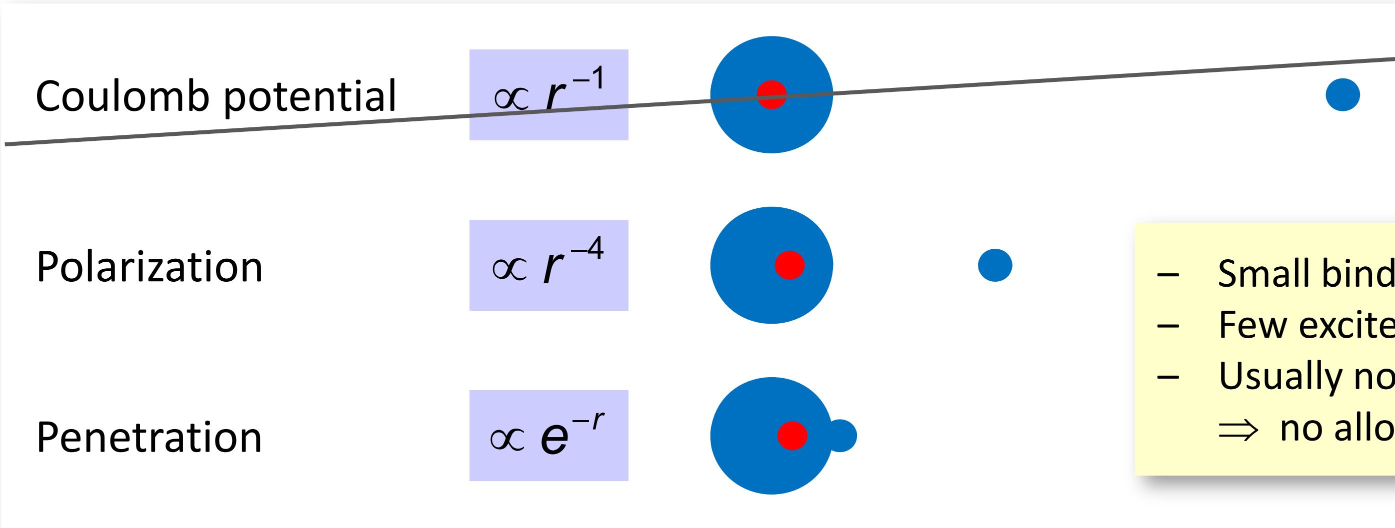

suspected in atomic anions

- Small binding energy
- Few excited states
- Usually no states with opposite parity
  $\Rightarrow$ no allowed transitions

- Known atomic anions with *opposite-parity* excited states

Os^-
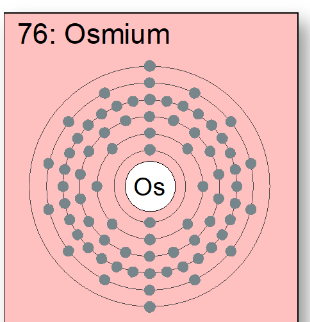

Ce^-
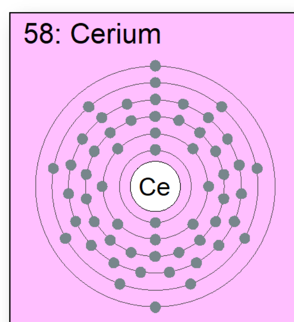

La^-
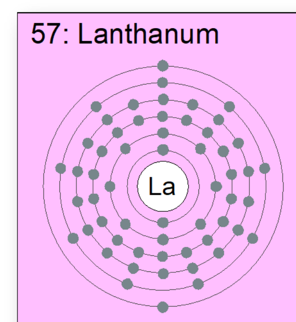

Anion formation and binding

- Binding in atomic systems:

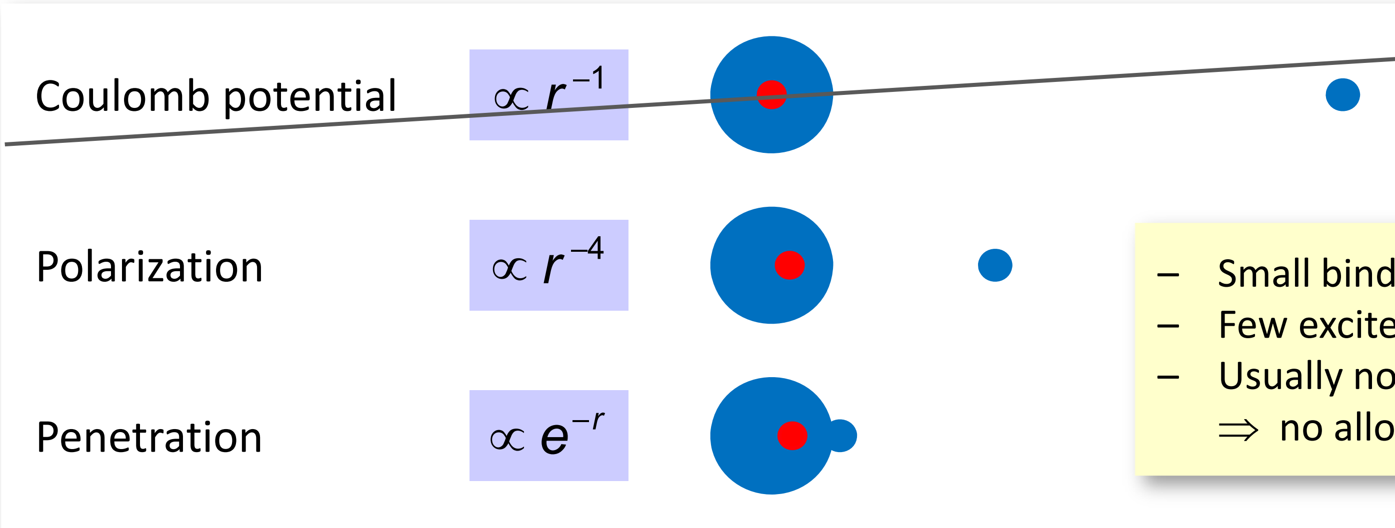

suspected in
atomic anions

- Small binding energy
- Few excited states
- Usually no states with opposite parity
  $\Rightarrow$ no allowed transitions

- Known atomic anions with *opposite-parity* excited states

Os^-

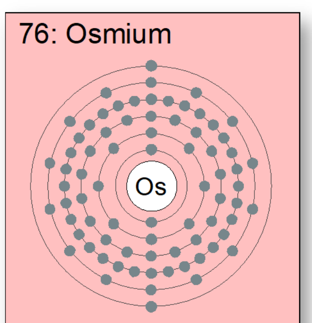

Ce^-

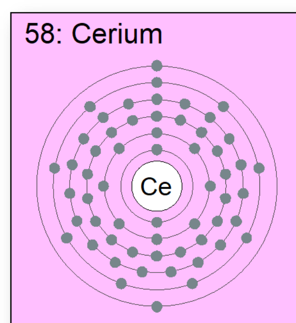

La^-

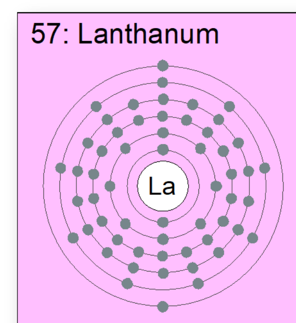

$\Gamma \approx 50$ Hz

Anion formation and binding

- Binding in atomic systems:

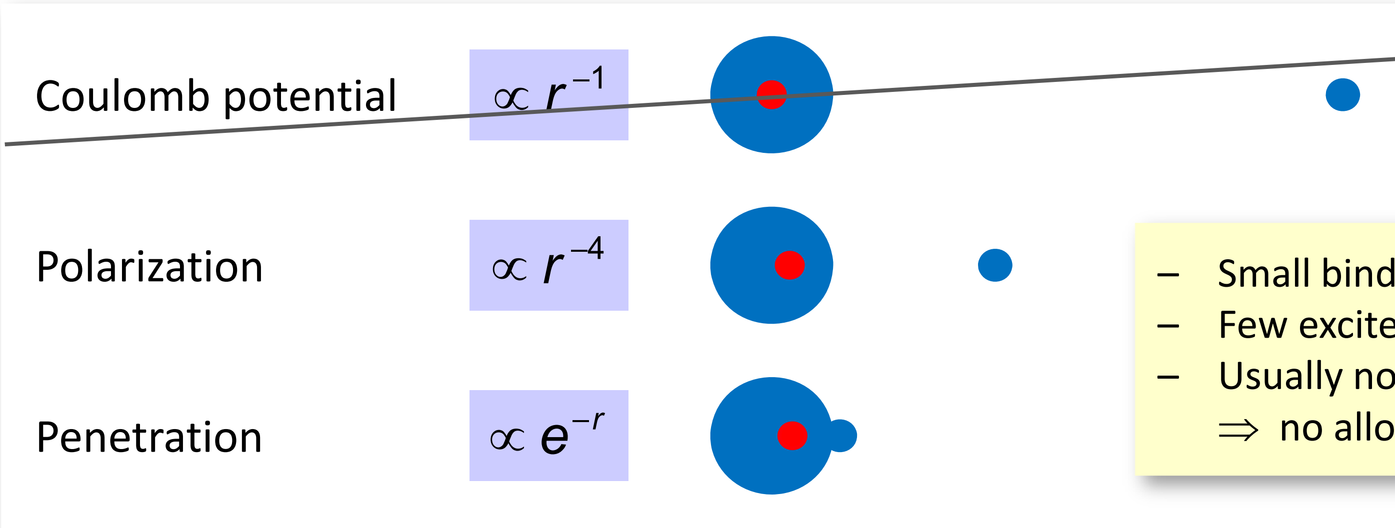

suppressed in atomic anions

- Small binding energy
- Few excited states
- Usually no states with opposite parity
  $\Rightarrow$ no allowed transitions

- Known atomic anions with *opposite-parity* excited states

Os^{-}

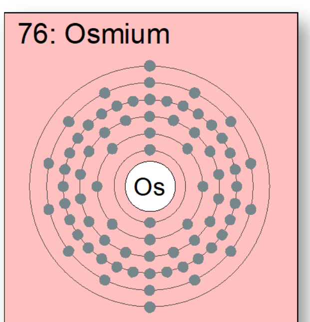

$\Gamma \approx 50$ Hz

Ce^{-}

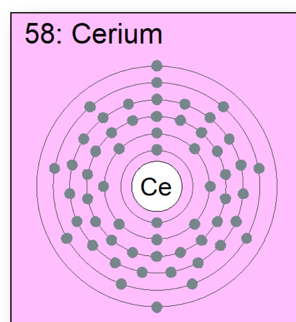

La^{-}

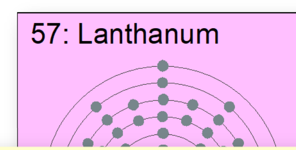

For a similar approach using molecular ions, see Julian Fesel's talk, Fri 10:20

Laser cooling candidate La⁻

- **2010**: Theoretical prediction of bound – bound transitions in La⁻:

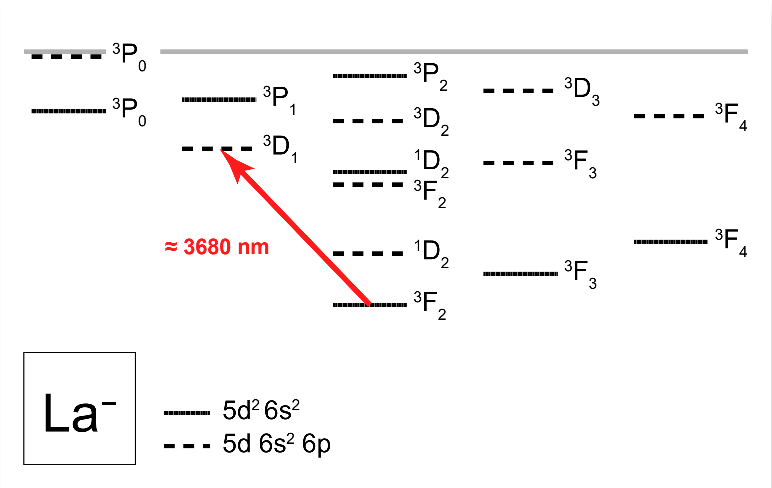

Transition rate $\Gamma \approx 4.5$ kHz

99.98% closed transition

[S. M. O'Malley & D. R. Beck, Phys. Rev. A **81** (2010) 032503]

- **2014**: Experimental demonstration:

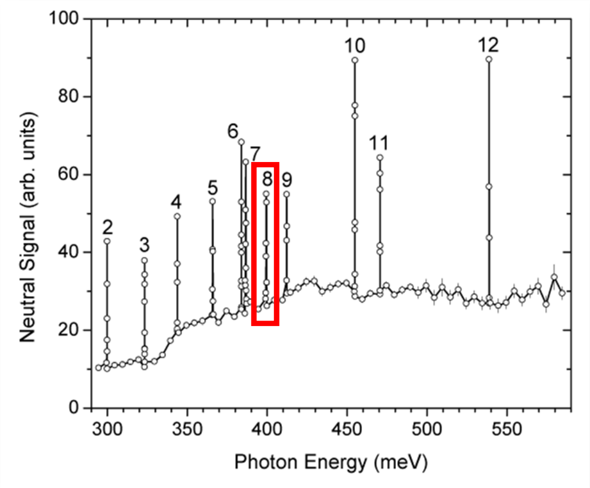

Laser spectroscopy with tunable OPO pumped by pulsed Nd:YAG

Peak 8

E = 399.42(3) meV

λ = 3104.4(2) nm

[C. W. Walter & N. D. Gibson, Phys. Rev. Lett. **113** (2014) 063001]

Laser spectroscopy setup

- Overall schematic

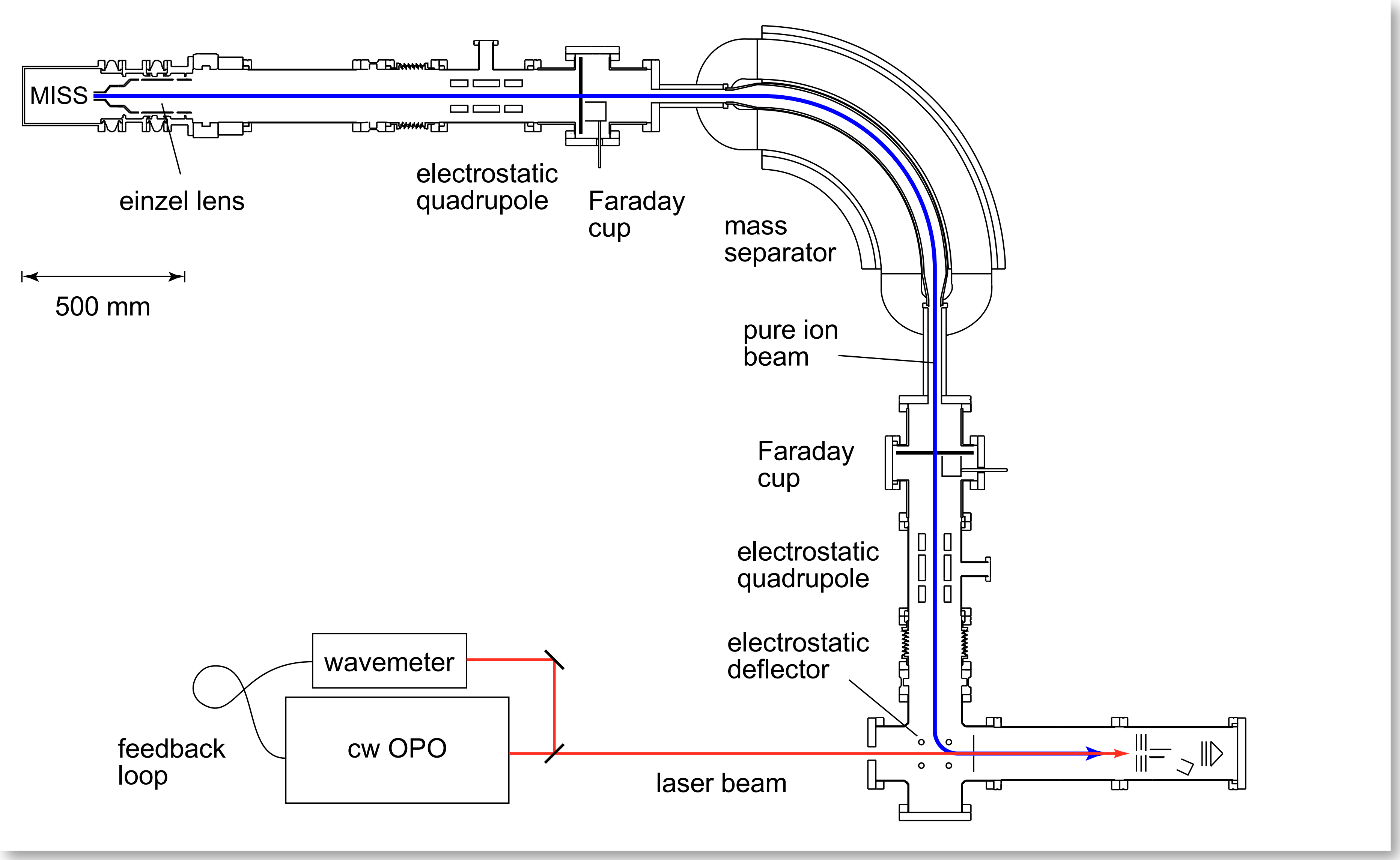

Laser spectroscopy setup

- Overall schematic
  - Ion production

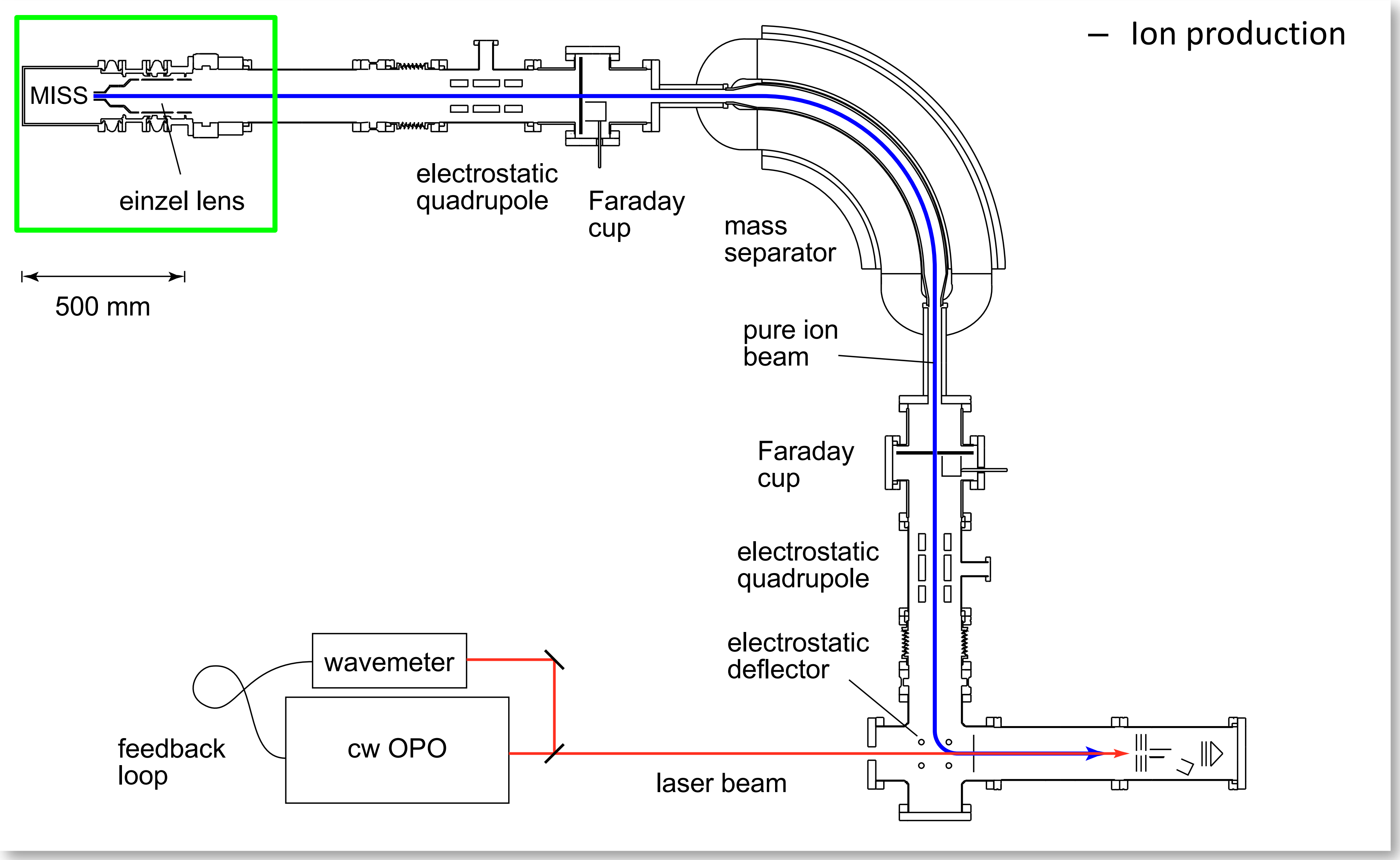

Laser spectroscopy setup

- Overall schematic

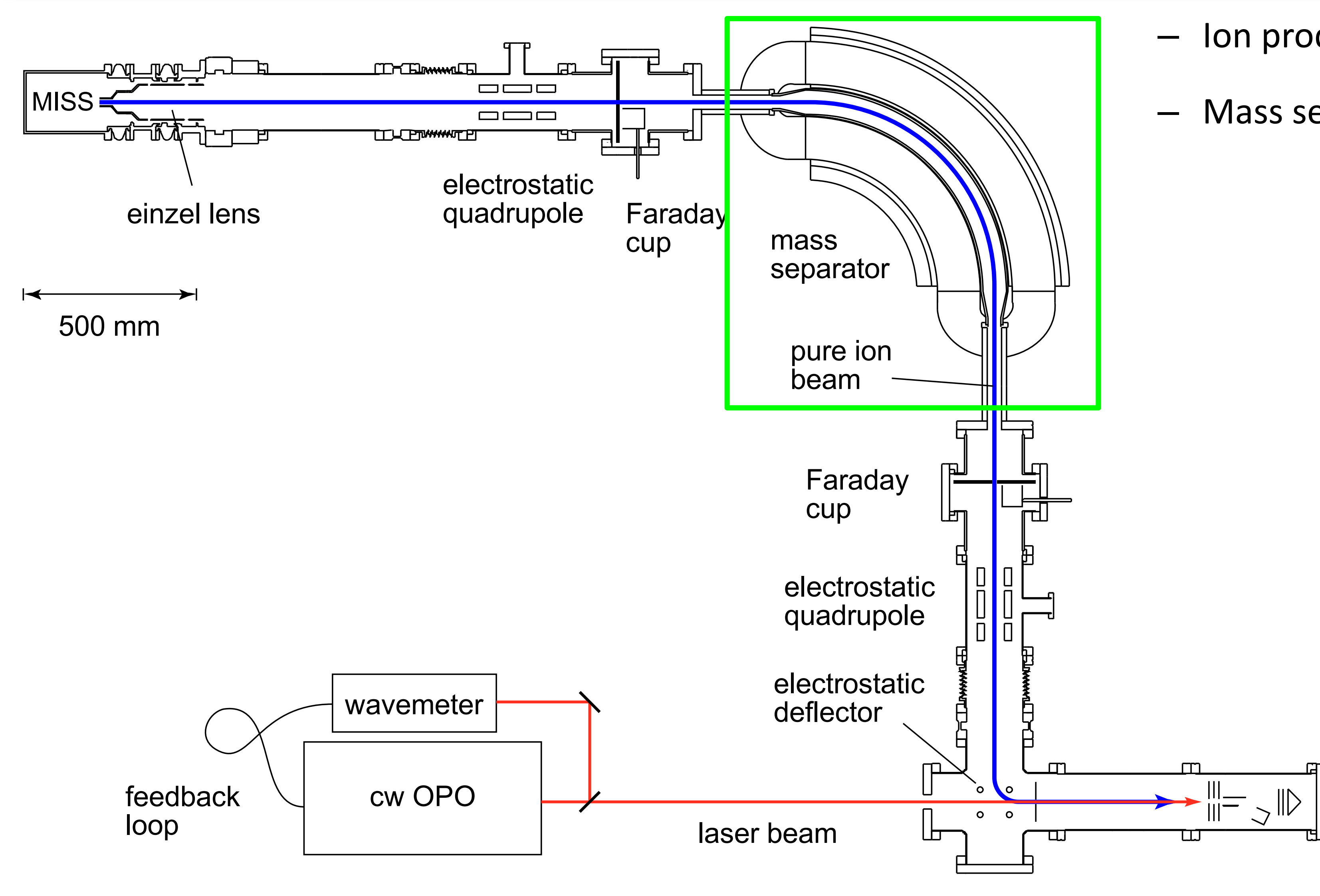

  - Ion production
  - Mass separation

Laser spectroscopy setup

- Overall schematic

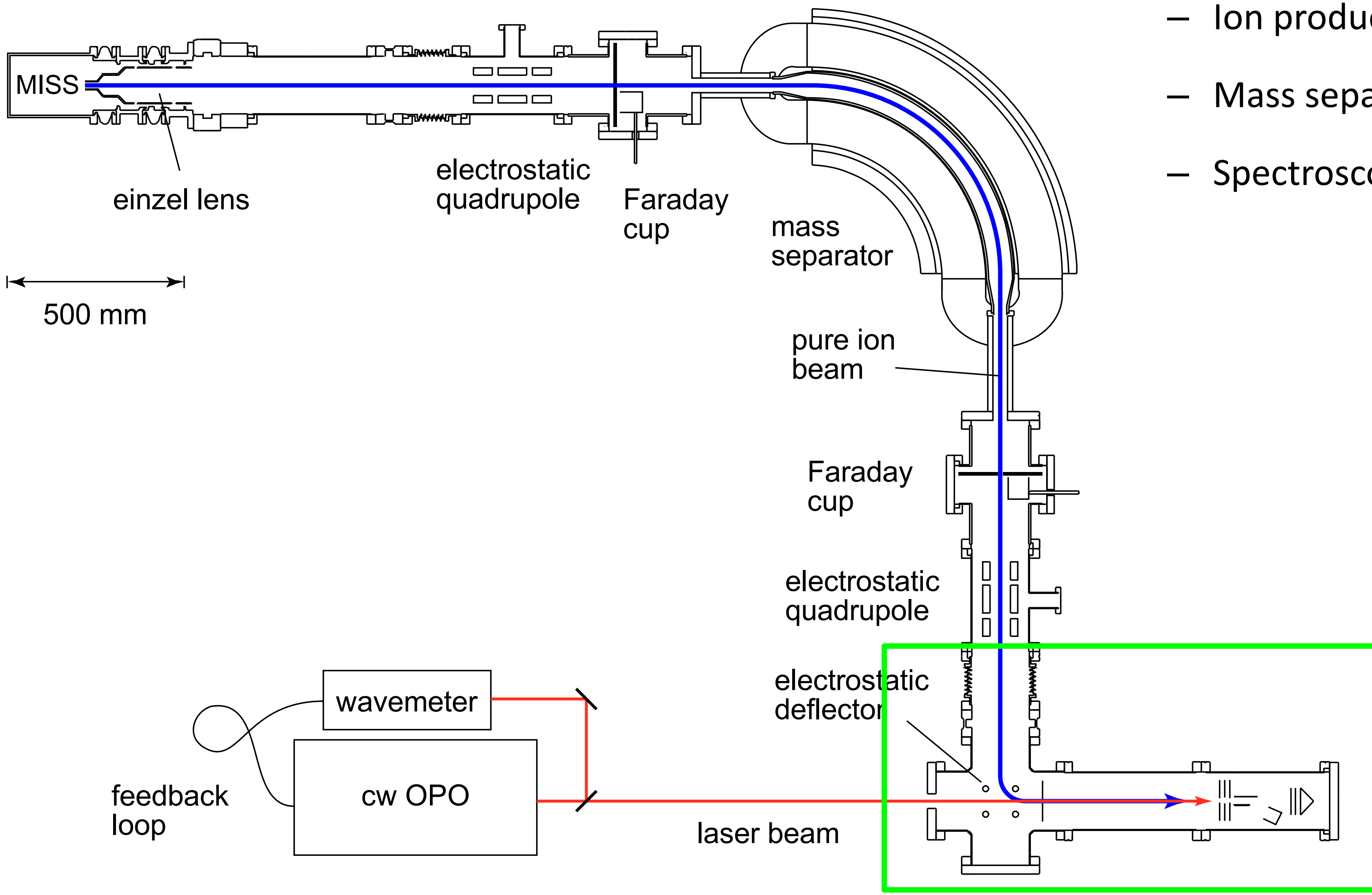

– Ion production
– Mass separation
– Spectroscopy

Laser spectroscopy / trap setup

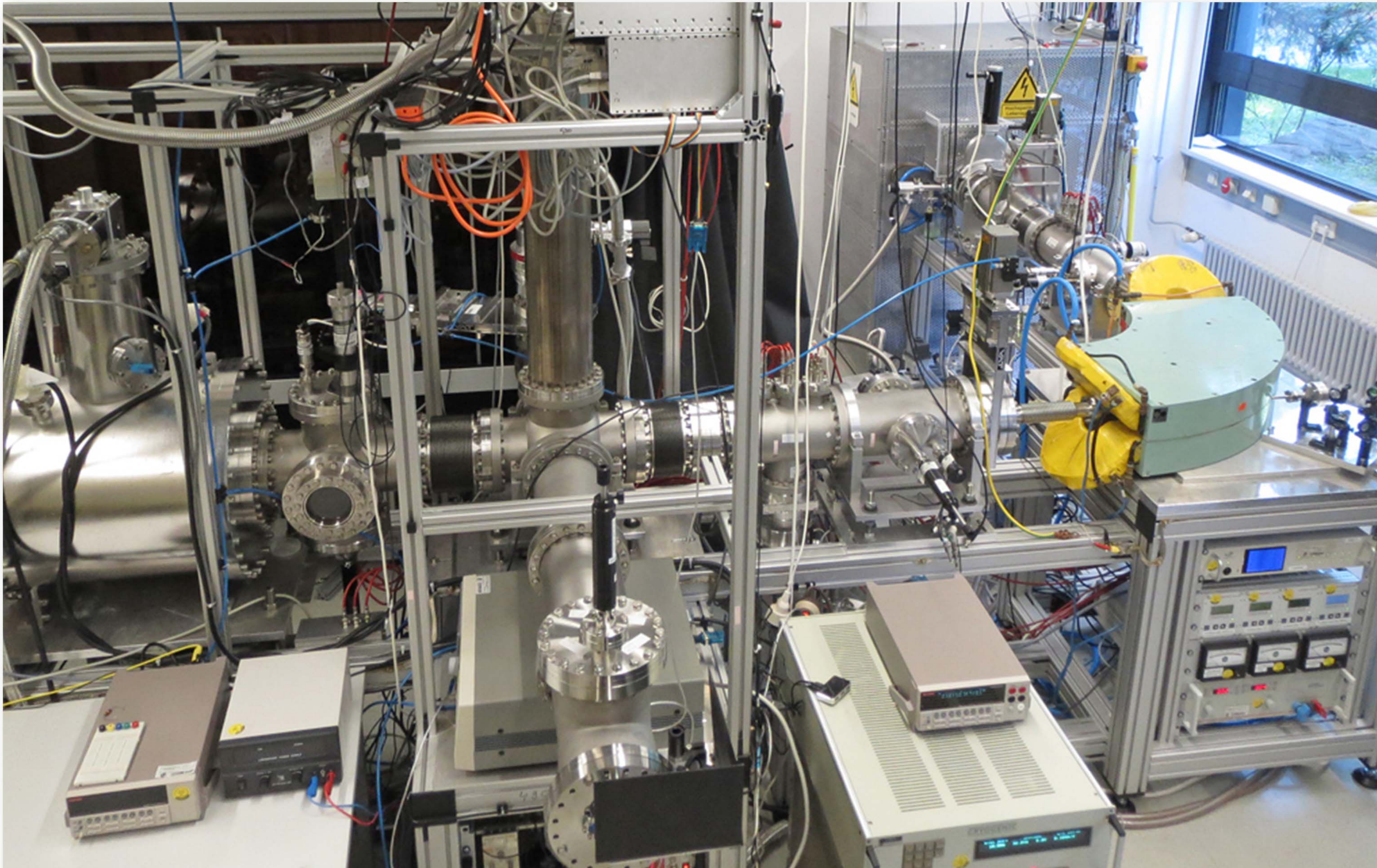

Collinear laser spectroscopy of La⁻

- Measurement principle

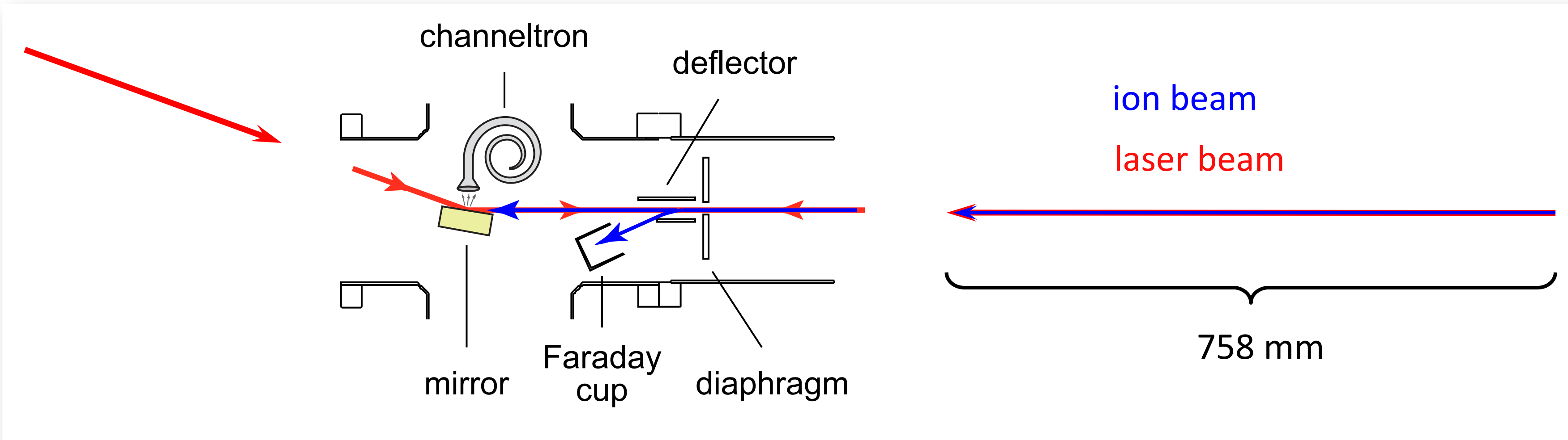

  - Ion beam and laser beam are superimposed
  - When laser in resonance, ions are excited, neutralized by photodetachment
  - Neutral atoms are detected on forward channeltron
  - 2nd laser anticollinear (out of resonance) to avoid power broadening

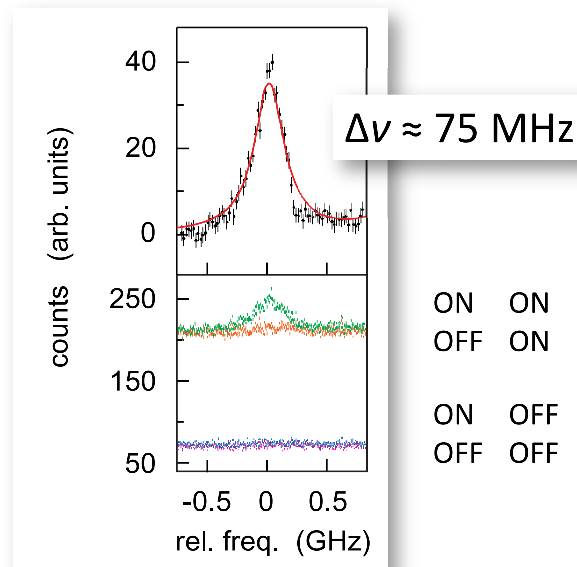

Hyperfine structure of La^{-}

- Resonance with resolved HFS (7 out of 9 peaks)

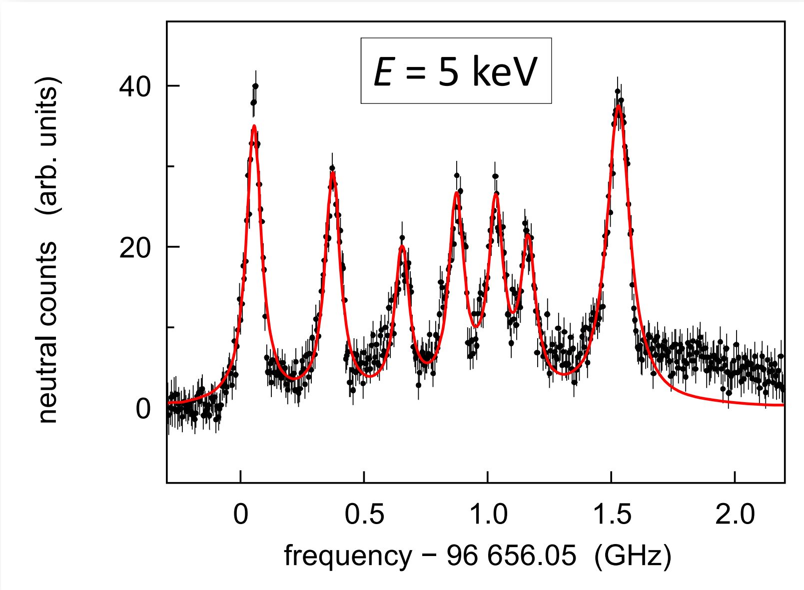

La139
7/2+
99.9

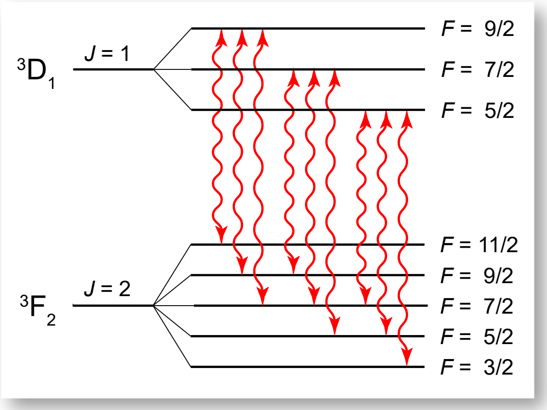

[E. Jordan *et al.*,
Phys. Rev. Lett. **115** (2015) 113001]

- 16 resonances recorded at beam energies ± 5…10 keV
- Center-of-mass frequency/wavelength determined from Doppler-corrected resonances:

ν = 96.592,80(10) THz
λ = 3.103,6729(32) µm

- Precision improved by factor ≈75, deviation 2σ

HFS coefficients

- Determination of A and B coefficients from fit

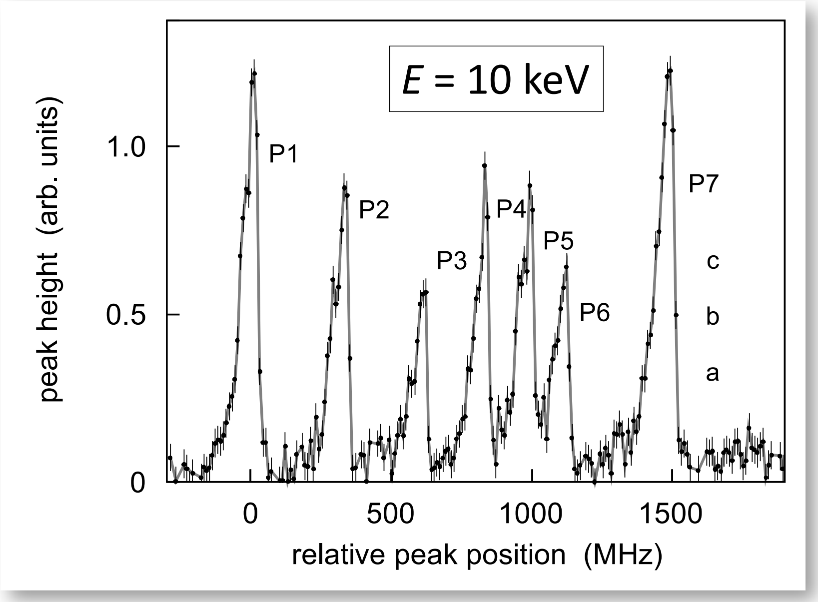

[E. Jordan *et al.*, Phys. Rev. Lett. **115** (2015) 113001]

Hyperfine splitting:

$$\Delta E_{M1+E2} = \frac{A}{2} C + \frac{B}{2} D$$

where *C*, *D* are functions of quantum numbers *I*, *J*, *F*

– Experimental HFS coefficients from fit to 9 best resonances

A_g = 146.8(3) MHz $\quad$ B_g = 36(9) MHz

A_e = 110.6(7) MHz $\quad$ B_e = 5(1) MHz

⇒ Unambiguous assignment of peaks to HFS transitions

(must fix relative heights for Peaks 7a–c to obtain their positions)

HFS coefficients

- Determination of A and B coefficients from fit

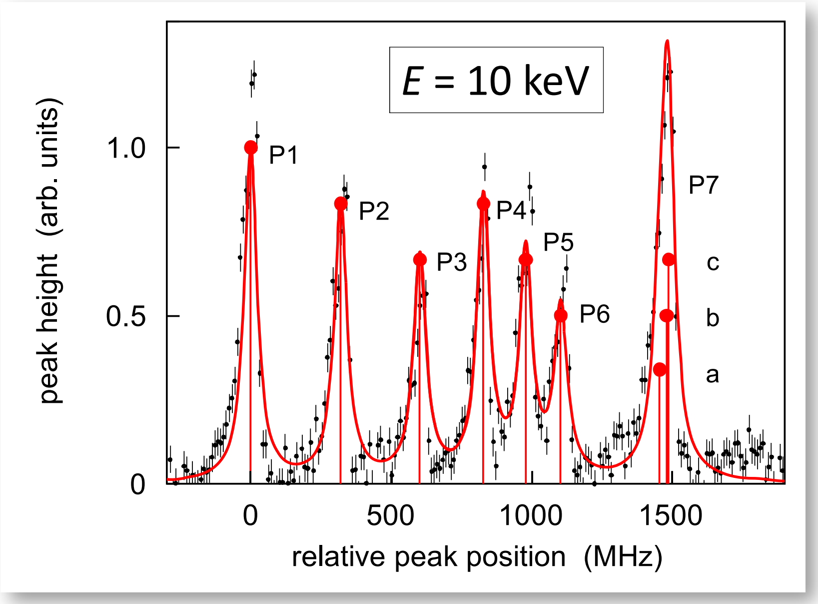

Hyperfine splitting:

$$\Delta E_{M1+E2} = \frac{A}{2} C + \frac{B}{2} D$$

where *C*, *D* are functions of quantum numbers *I*, *J*, *F*

[E. Jordan *et al.*, Phys. Rev. Lett. **115** (2015) 113001]

– Experimental HFS coefficients from fit to 9 best resonances

A_g = 146.8(3) MHz	B_g = 36(9) MHz
A_e = 110.6(7) MHz	B_e = 5(1) MHz

$\Rightarrow$ Unambiguous assignment of peaks to HFS transitions

(must fix relative heights for Peaks 7a–c to obtain their positions)

La⁻ laser cooling scheme

- HFS energy level diagram (no magnetic field)

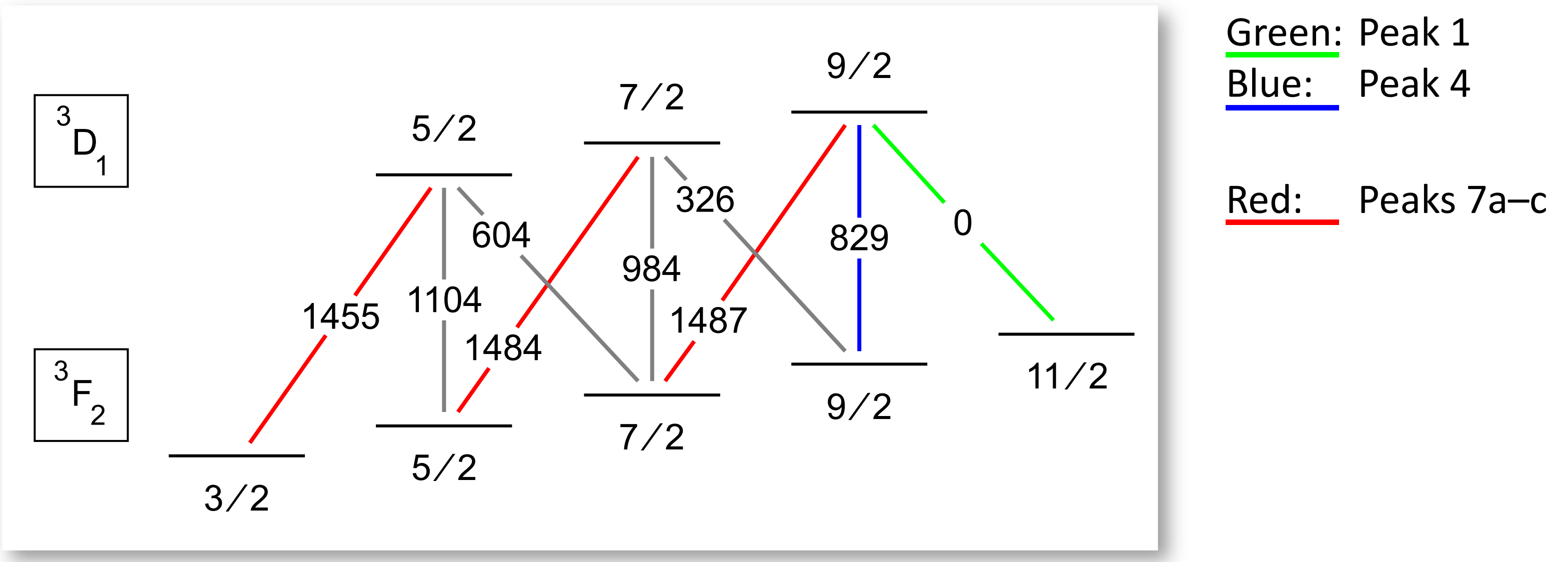

- Cooling with $F = 11/2 \rightarrow 9/2$ transition (Peak 1)
  $\Delta F = 0, -1$ decays must be repumped
- Only three laser frequencies required (3rd laser > 40 MHz)
  → Sideband generation by EOMs implemented
- Initially work in **Paul trap** to avoid additional Zeeman splitting

Cross-section measurement

- Combined transverse/collinear spectroscopy:

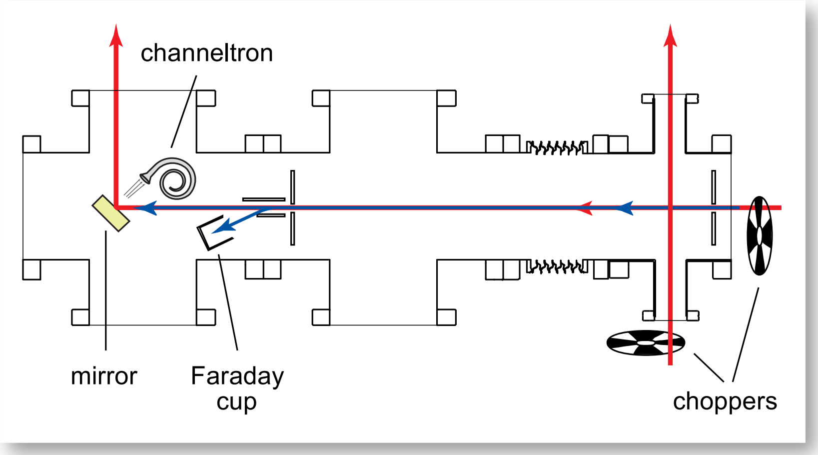

$$\dot{N}_g = -\sigma_0 \varphi N_g + (\sigma_0 \varphi + \tau^{-1}) N_e$$

$$\dot{N}_e = \sigma_0 \varphi N_g - (\sigma_0 \varphi + \tau^{-1} + \sigma_d \varphi) N_e$$

$$\dot{N}_d = \sigma_d \varphi N_e$$

σ_0, σ_d – excited / detached cross-section
τ – lifetime of excited state
φ – photon flux

– rate equation for ground, excited state and detached populations
– analytical expressions for N_e, N_d
measured: N_d
– resonant cross-section:

$\sigma_0 = 1.0(1) \times 10^{-12}$ cm^2

$\Gamma \approx 9.7$ kHz

(factor 200 higher than in Os$^-$)

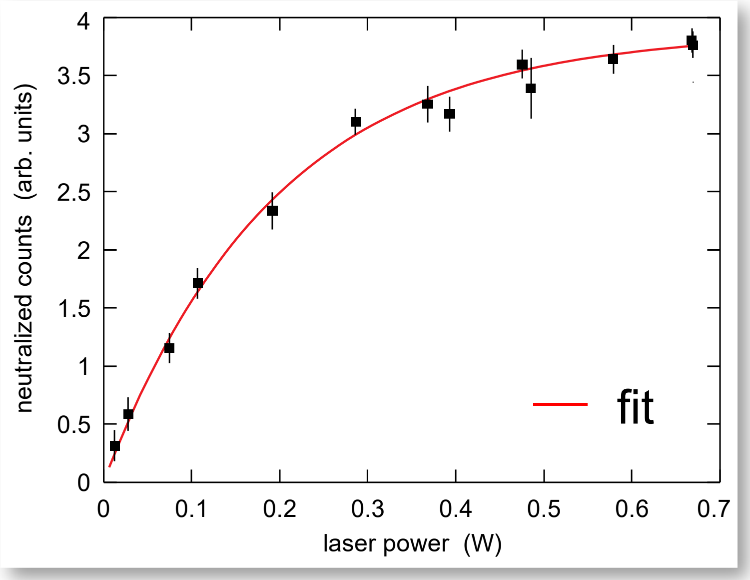

[G. Cerchiari *et al.*, accepted for publ. in Phys. Rev. Lett.]

Decay rates and branching ratios

- Calculation of decay rates and branching ratios by hybrid CI+MBPT method

Upper level	Lower level	*A* (1/s)	Branching r.
$^3D_1^o$	$^3F_2^e$	45 400	0.999974
	$^1D_2^e$	1.18	0.000026
$^1D_2^e$	$^1D_2^o$	1.95	0.956
	$^3F_2^e$	0.09	0.044
$^1D_2^o$	$^3F_2^e$	168	0.791
	$^3F_3^e$	44.4	0.209
$^3F_3^e$	$^3F_2^e$	0.00756	1.0
$^3D_2^o$	$^3F_2^e$	4 500	0.1059
	$^3F_3^e$	37 900	0.8924
	$^1D_2^e$	44.1	0.0010
	$^3P_1^e$	27.5	0.0006

⇒ Full information on cooling cycle

[G. Cerchiari *et al.*, accepted for publ. in Phys. Rev. Lett.]

Decay rates and branching ratios

- Calculation of decay rates and branching ratios by hybrid CI+MBPT method

experimental:
A = 49 000(5000) 1/s

Upper level	Lower level	A (1/s)	Branching r.
$^3D_1^o$	$^3F_2^e$	45 400	0.999974
	$^1D_2^e$	1.18	0.000026
$^1D_2^e$	$^1D_2^o$	1.95	0.956
	$^3F_2^e$	0.09	0.044
$^1D_2^o$	$^3F_2^e$	168	0.791
	$^3F_3^e$	44.4	0.209
$^3F_3^e$	$^3F_2^e$	0.00756	1.0
$^3D_2^o$	$^3F_2^e$	4 500	0.1059
	$^3F_3^e$	37 900	0.8924
	$^1D_2^e$	44.1	0.0010
	$^3P_1^e$	27.5	0.0006

$\Rightarrow$ Full information on cooling cycle

[G. Cerchiari *et al.*, accepted for publ. in Phys. Rev. Lett.]

Decay rates and branching ratios

- Calculation of decay rates and branching ratios by hybrid CI+MBPT method

experimental:
A = 49 000(5000) 1/s

Upper level	Lower level	A (1/s)	Branching r.
$^3D_1^o$	$^3F_2^e$	45 400	0.999974
	$^1D_2^e$	1.18	0.000026
$^1D_2^e$	$^1D_2^o$	1.95	0.956
	$^3F_2^e$	0.09	0.044
$^1D_2^o$	$^3F_2^e$	168	0.791
	$^3F_3^e$	44.4	0.209
$^3F_3^e$	$^3F_2^e$	0.00756	1.0
$^3D_2^o$	$^3F_2^e$	4 500	0.1059
	$^3F_3^e$	37 900	0.8924
	$^1D_2^e$	44.1	0.0010
	$^3P_1^e$	27.5	0.0006

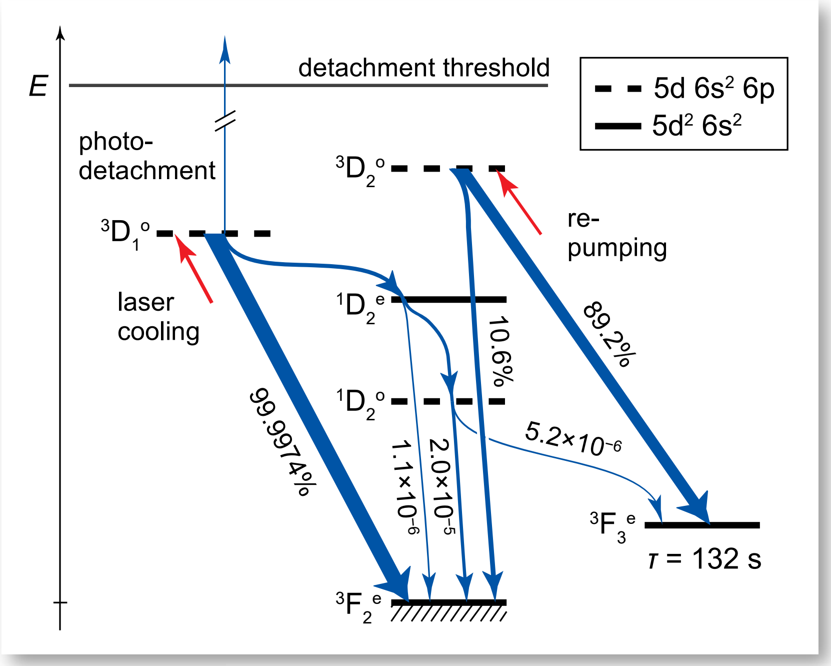

λ = 3.104 µm

λ = 3.207 µm

$\Rightarrow$ Full information on cooling cycle

[G. Cerchiari *et al.*, accepted for publ. in Phys. Rev. Lett.]

Discussion

- 1D Doppler laser cooling:
  - Doppler temperature T_D = 0.17 µK
  - cooling from 100 K to T_D requires scattering of ≈ 8.4×10^4 photons ⇒ cooling time 3.7 s
  - after cooling, 40% of ions in metastable 'dark' state $^3F_3{}^e$, 10% photodetached
  - if necessary, $^3F_3{}^e$ state can be repumped

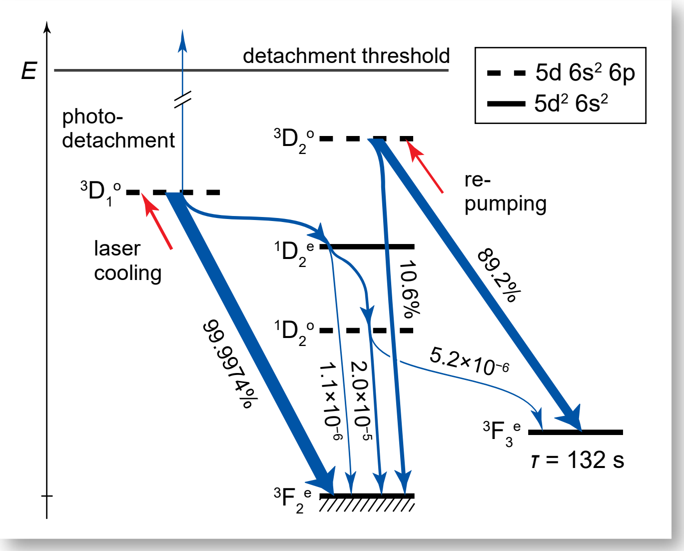

- Strategy towards demonstration of laser cooling:
  - must reach starting temperature of ≈ 100 K
  - in Penning trap, easily achieved by electron cooling
  - in Paul trap, need new cooling mechanism
    - buffer gas cooling
    - "laser-assisted evaporative cooling"

      [A. Crubellier, J. Phys. B **23** (1990) 3585]

Trapping and cooling anions

- Paul trap implemented downstream of spectroscopy section
  - linear RF quadrupole, 5 axial segments
  - radial and axial (oblique) laser access
  - MCP with phosphor screen as diagnostics for axial and transverse phase space

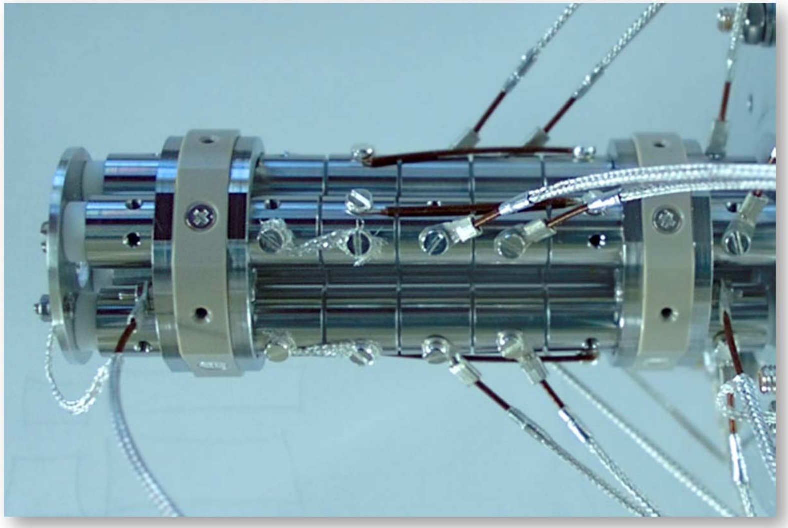

- Trap commissioned and characterized with Au^-/O^- ions:
  - max. number of ions loaded $\approx 10^5 \ldots 10^7$
  - storage time constant > min
  - laser-assisted evaporative cooling of O^-
    - geometrically selective neutralization with green laser (200 mW @ 532 nm)
    - velocity selection observed

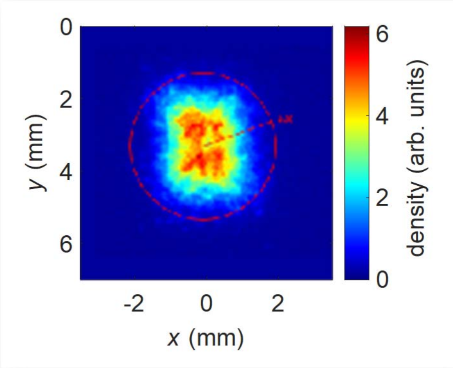

t = 60 s

Trapping and cooling anions

- Paul trap implemented downstream of spectroscopy section
  - linear RF quadrupole, 5 axial segments
  - radial and axial (oblique) laser access
  - MCP with phosphor screen as diagnostics for axial and transverse phase space

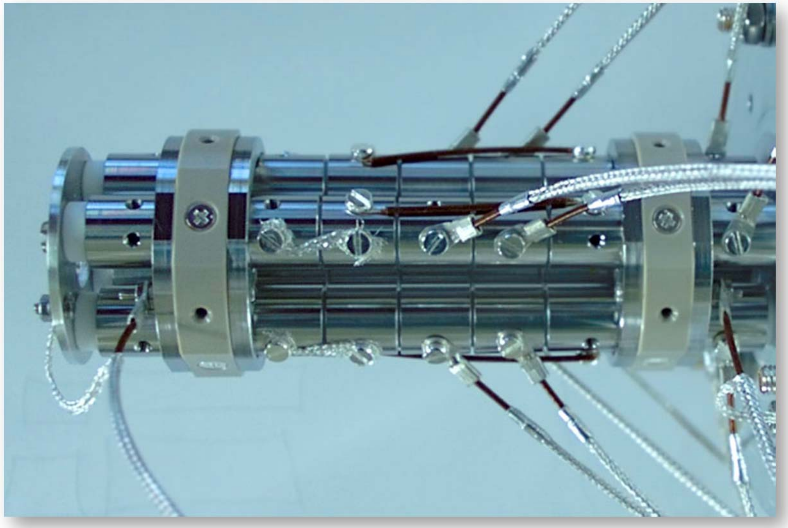

- Trap commissioned and characterized with Au^-/O^- ions:
  - max. number of ions loaded ≈ $10^5 \ldots 10^7$
  - storage time constant > min
  - laser-assisted evaporative cooling of O^-
    - geometrically selective neutralization with green laser (200 mW @ 532 nm)
    - velocity selection observed

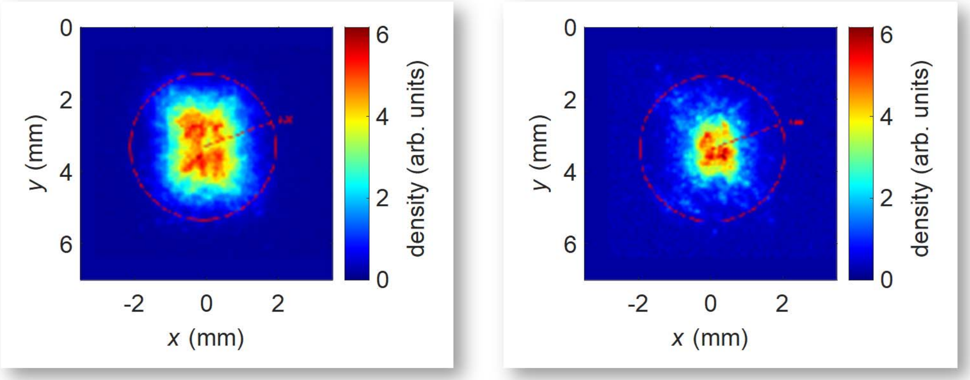

t = 60 s　　*t* = 65 s

preliminary

Conclusions

- Laser cooling of anions is a promising route to ultracold ensembles of negative ions
- Only few atomic anions exhibit suitable bound–bound transitions
- We have been investigating Os^- and La^- by optical spectroscopy to check their suitability for laser cooling
- La^- is a promising candidate – attempt to laser-cool anions in a Paul trap ongoing

Acknowledgments

- Team:

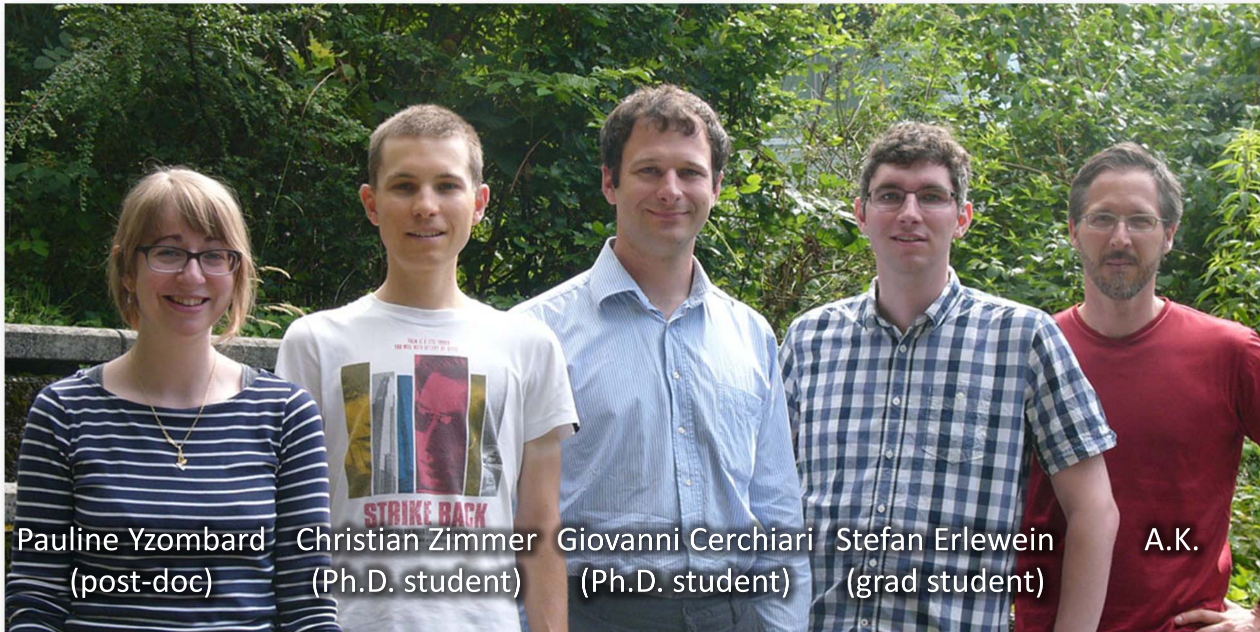

- Collaboration:
  Dag Hanstorp (Gothenburg U)
  Wesley Walter, Daniel Gibson (Denison U Ohio)
  Stephan Fritzsche (Helmholtz Institute and U Jena)
  Marianna Safronova (U of Delaware)

- Funding:
  Emmy Noether Programme DFG
  erc European Research Council

Extra slides

Anion formation and structure

- Atomic anions form by "partial same-shell shielding"
  - Valence electrons only partially shield nuclear charge

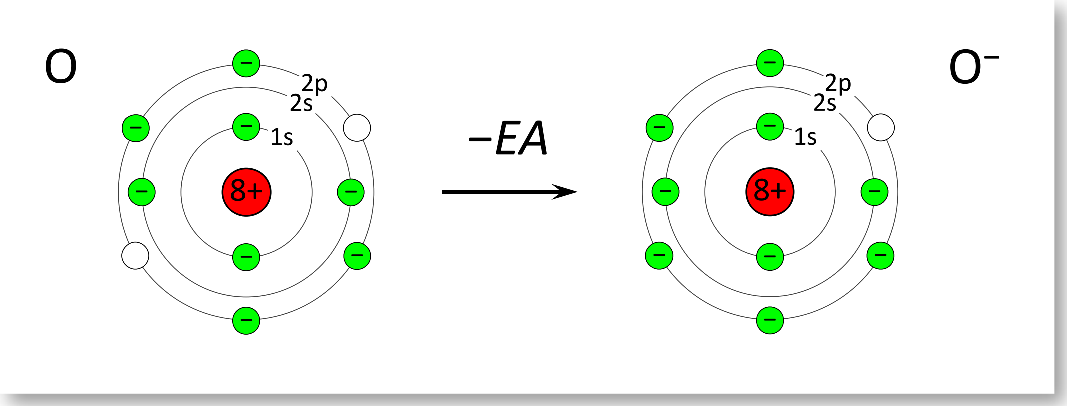

Oxygen anion electron affinity: 1.46 eV

- Differences compared to neutral atoms and cations:
  - Effect of Coulomb potential (r^{-1}) reduced
  - Main binding by (induced) short-ranged dipole potential (r^{-4})
  - Contribution by correlation (quantum mechanical effect)

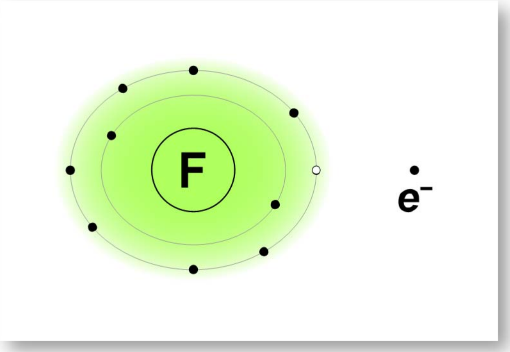

⇒ Few (or no) bound excited states

Anion formation and structure

- Atomic anions form by “partial same-shell shielding”
  - Valence electrons only partially shield nuclear charge

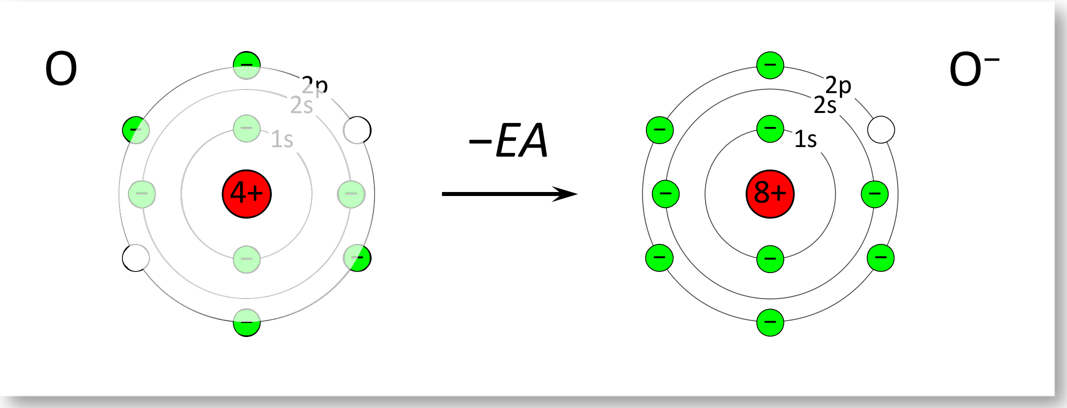

Oxygen anion
electron affinity:
1.46 eV

- Differences compared to neutral atoms and cations:
  - Effect of Coulomb potential (r^{-1}) reduced
  - Main binding by (induced) short-ranged dipole potential (r^{-4})
  - Contribution by correlation (quantum mechanical effect)

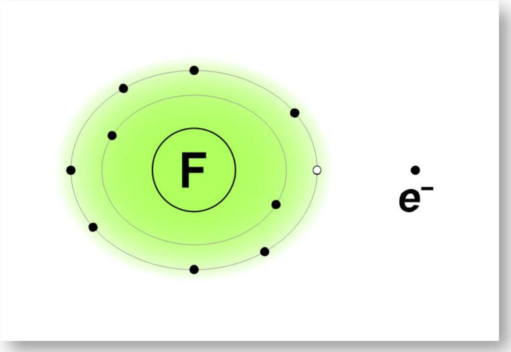

⇒ Few (or no) bound excited states

Laser cooling candidate Os^-

- Potential laser cooling transition:

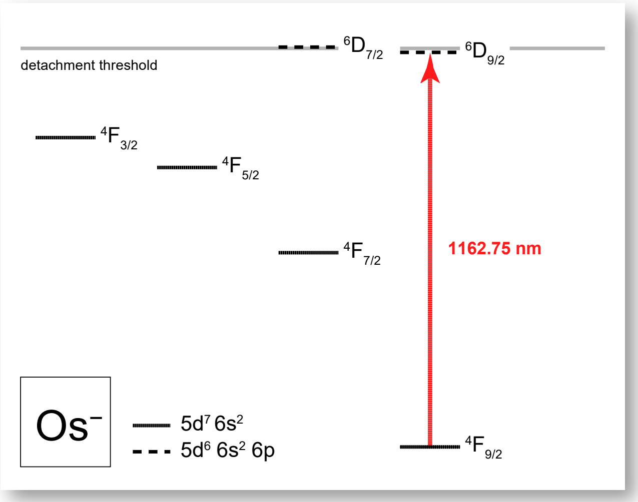

Wavelength	λ = 1162.7 nm
Transition rate	Γ = 1…10 kHz (initial measurement)

[P. L. Norquist & D. R. Beck, Phys. Rev. A **61** (1999/2000) 014501;
R. C. Bilodeau & H. K. Haugen, Phys. Rev. Lett. **85** (2000) 534]

Os183	Os184	Os185	Os186	Os187	Os188	Os189	Os190	Os191	Os192	Os193
13.0 h		93.6 d						15.4 d		30.5 h
9/2+	0+	1/2-	0+	1/2-	0+	3/2-	0+	9/2-	0+	3/2-
	0.02		1.58	1.6	13.3	16.1	26.4		41.0	

- Experimental results:
  - Transition frequency confirmed
  - Cross-section / rate of resonant transition and photodetachment ⇒ 50 Hz
  - Hyperfine structure in $^{187}Os^-$, $^{189}Os^-$
  - Zeeman splitting in $^{192}Os^-$ in external magnetic field

} First-ever measurements in atomic anions

[U. Warring *et al.*, Phys. Rev. Lett. **102** (2009) 043001;
A. Fischer *et al.*, Phys. Rev. Lett. **104** (2010) 073004;
A.K. *et al.*, Phys. Rev. A **89** (2014) 043430]

Indirect laser cooling of negative ions

- Principle:

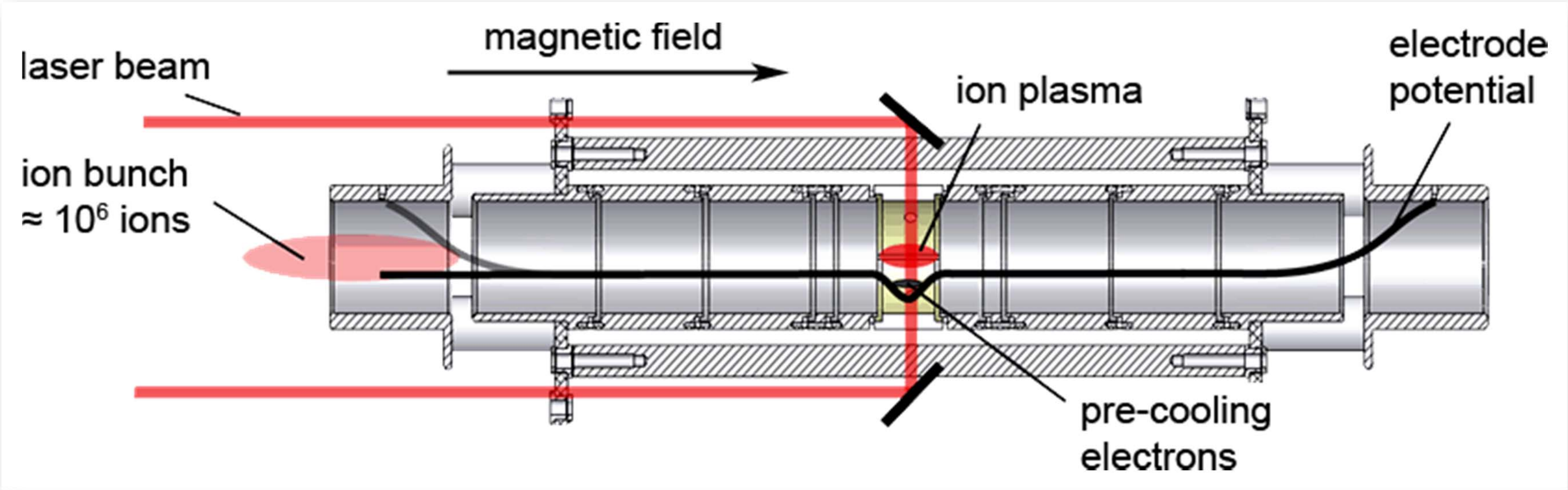

1. Capture anion bunch in Penning trap
2. Pre-cool anions with electrons
3. Laser-cool the anions
4. Simultaneously load other ions into trap
5. Sympathetically cool them with laser-cooled anions

[A. K. & J. Walz, New J. Phys. **8** (2006) 45]

Spectroscopy setup for La⁻

- Laser beam setup

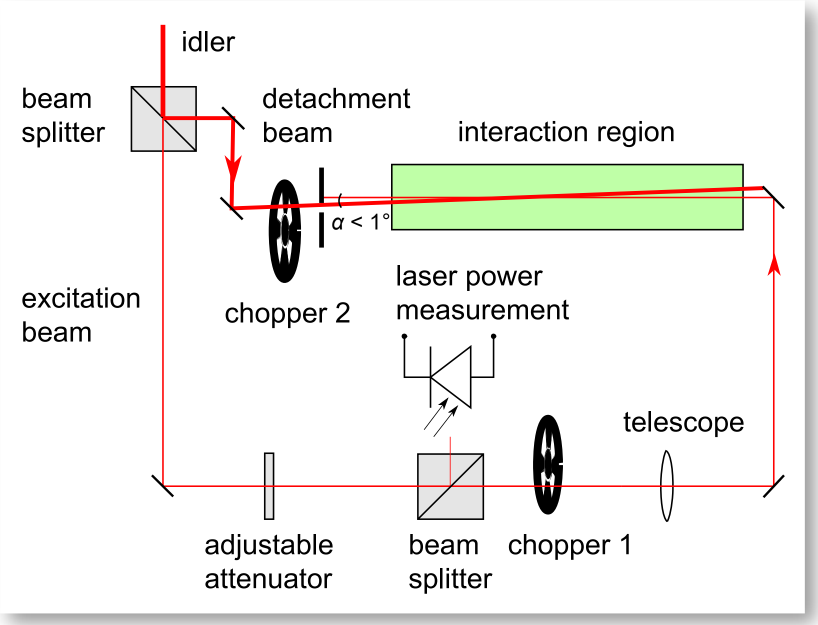

Laser powers:

- Excitation: 2…60 mW
- Detachment: ≈ 1 W

Repetition frequencies:

- Chopper 1: 50 Hz
- Chopper 2: 5 Hz

- Subtracted background signals
  - OFF–ON: Ions arriving in interaction region in excited state
  - ON–OFF: Two-photon detachment by excitation laser only
  - OFF–OFF: Ions neutralized by other mechanisms (*e.g.* residual gas)

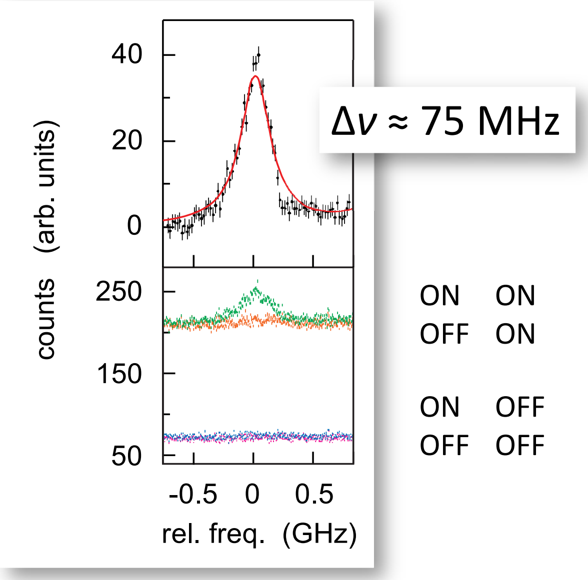

Ion production

- Negative-ion source
  - Middleton-type ion source: Sputtering of Cs^+ ions onto surface of desired target material

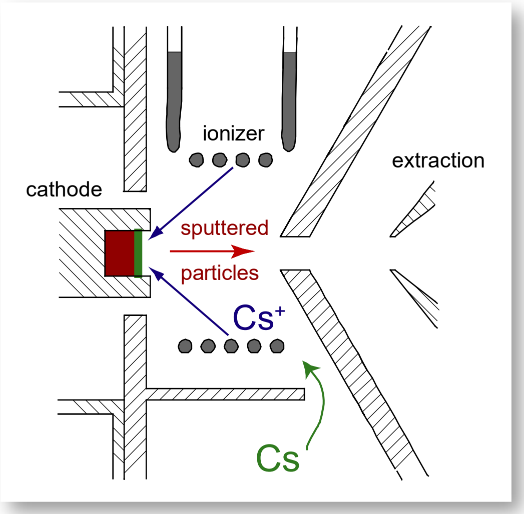

[R. Middleton, NIM **214** (1983) 139]

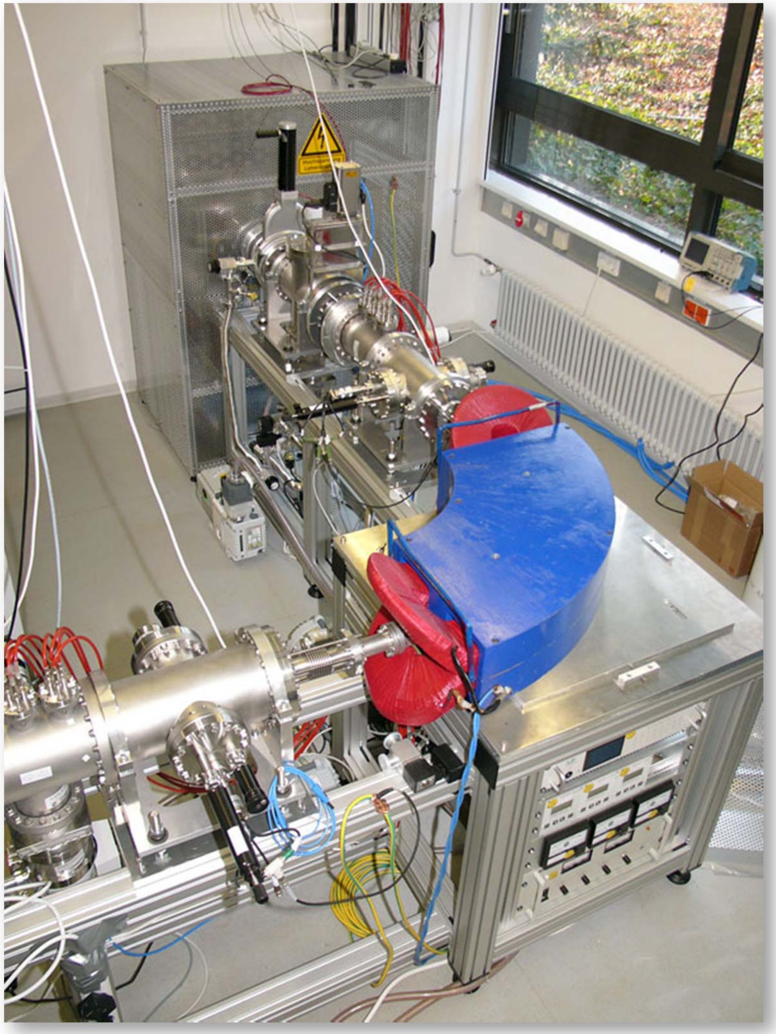

  - Typical ion source performance: several 100 nA of $^{192}Os^-$
  - Mass resolving power: $R \approx 180$

$\Rightarrow$ $^{192}Os^-$ can be separated from nearest isotope $^{190}Os^-$

Ion production

- Negative-ion source
  - Middleton-type ion source: Sputtering of Cs^+ ions onto surface of desired target material

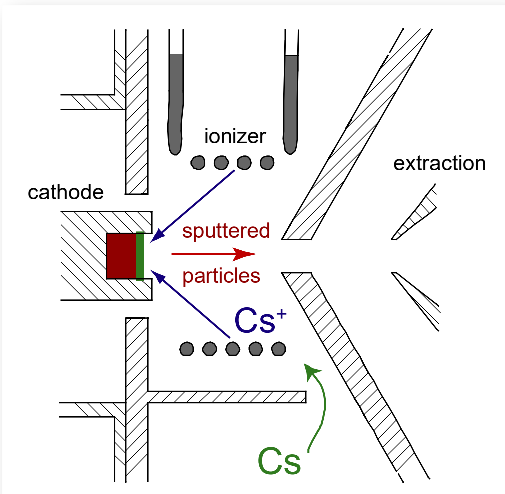

[R. Middleton, NIM **214** (1983) 139]

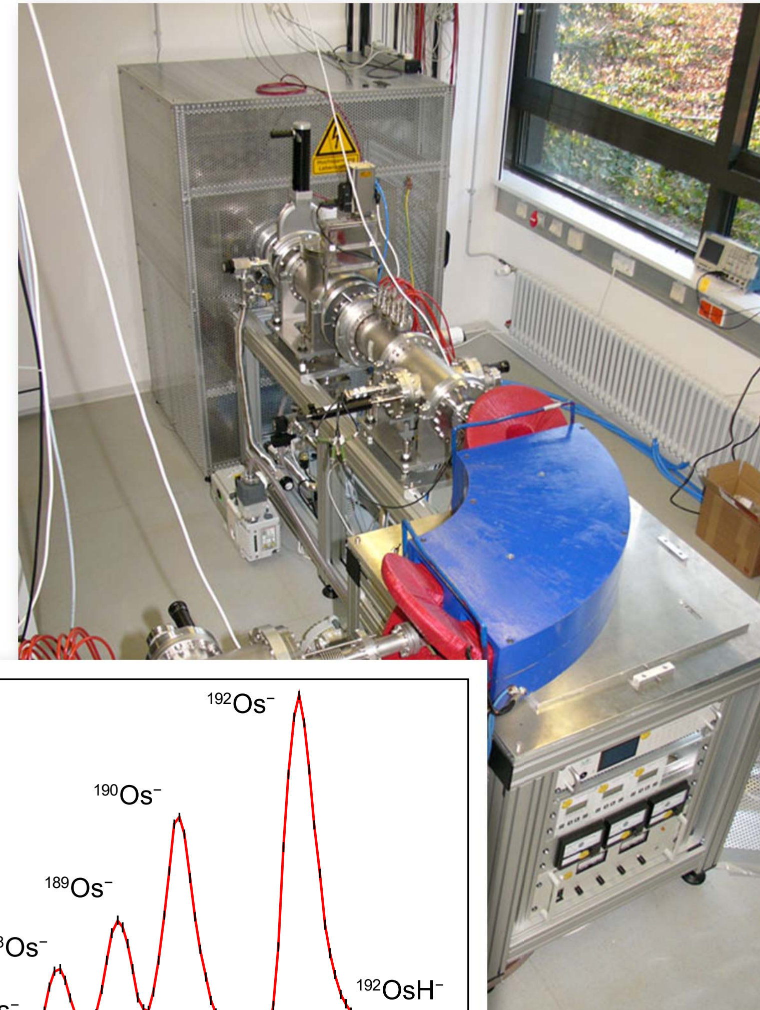

  - Typical ion source performance: several 100 nA of $^{192}Os^-$
  - Mass resolving power: $R \approx 180$

  $\Rightarrow$ $^{192}Os^-$ can be separated from nearest isotope $^{190}Os^-$

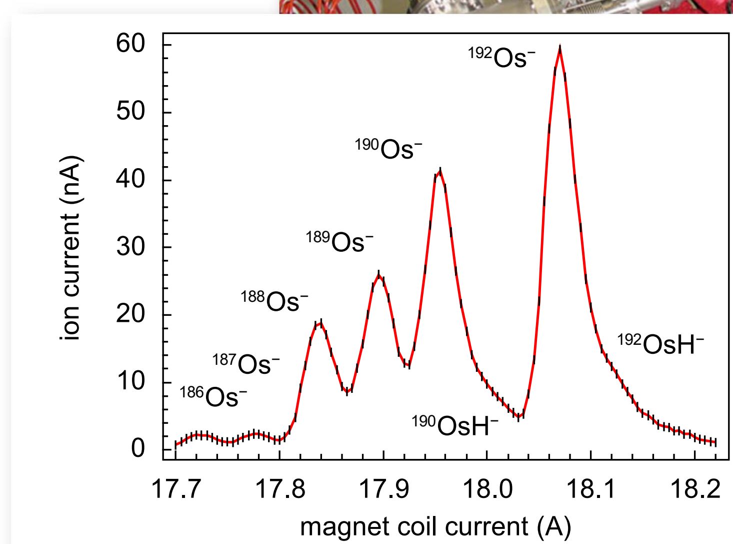

Laser system for La⁻ spectroscopy

- cw-OPO laser seeded by DFB fiber laser:

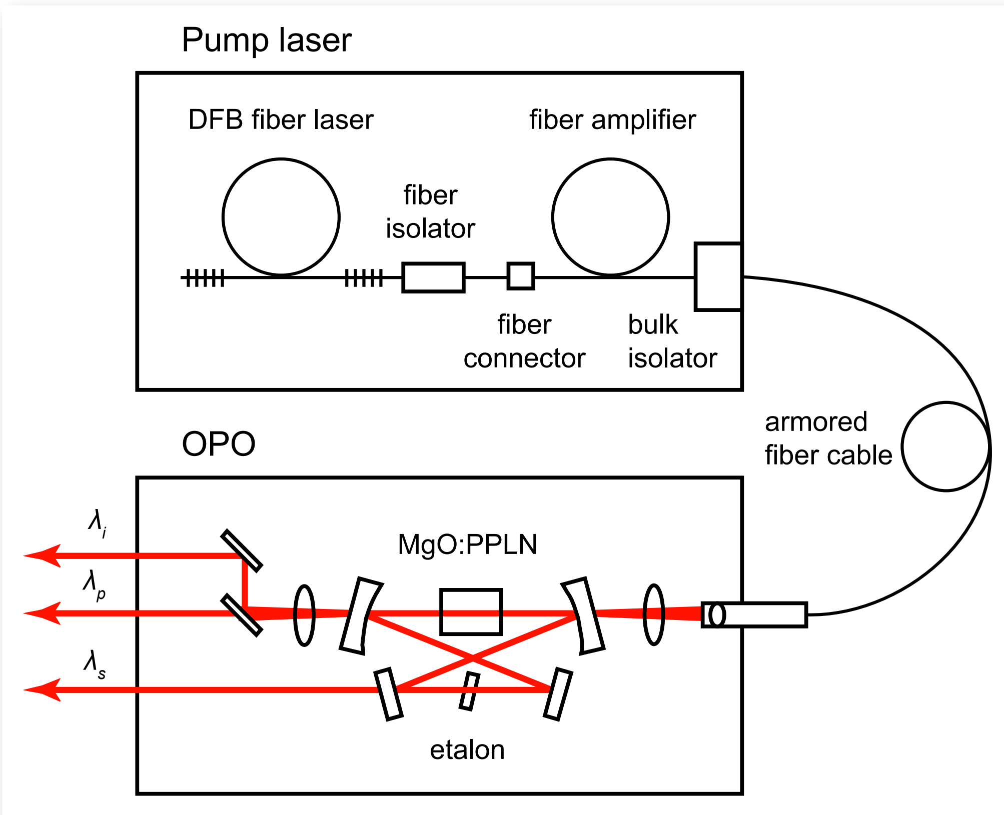

λ = 2.5…3.2 µm

P > 600 mW

Γ < 1 MHz

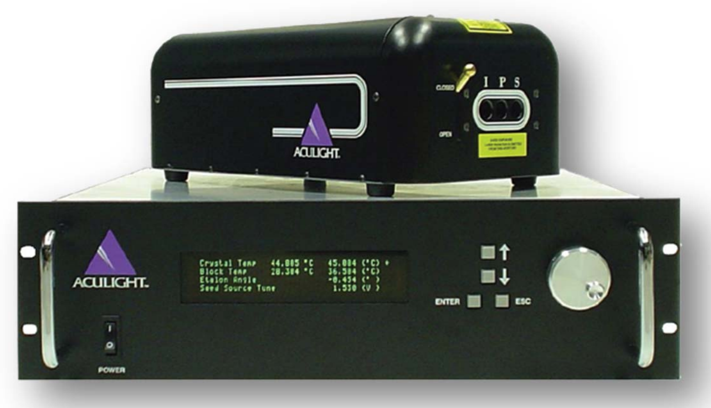

Aculight Argos SF10

Doppler correction of peak frequencies

- Doppler shift as a function of ion velocity/energy:

$$f = f_0 \sqrt{\frac{c + v(E)}{c - v(E)}}$$

- Frequencies for Peaks 1–7 from parabola:

Peak	Rel. intensity	Frequency (MHz)
1	1.00(11)	0.0(5.8)
2	0.77(8)	324.8(5.8)
3	0.51(6)	604.1(5.9)
4	0.81(8)	825.1(5.8)
5	0.74(8)	990.1(5.9)
6	0.53(7)	1116.2(6.1)
7	1.08(10)	1480.2(5.8)

[relative to Peak 1
at 96.592,004(80) THz]

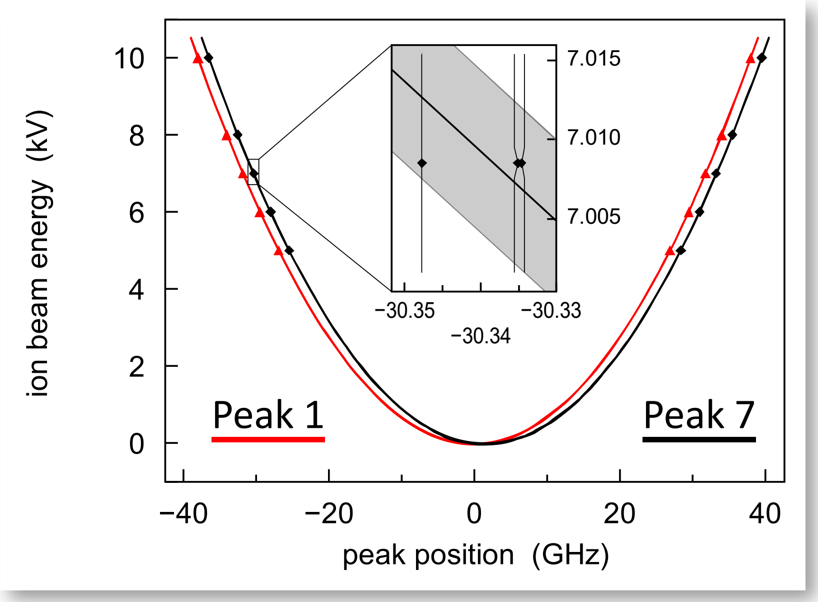

[E. Jordan *et al.*,
Phys. Rev. Lett. **115** (2015) 113001]

La⁻ in a magnetic field

- Zeeman splitting (B << 1 T)

  Transition splits 192-fold

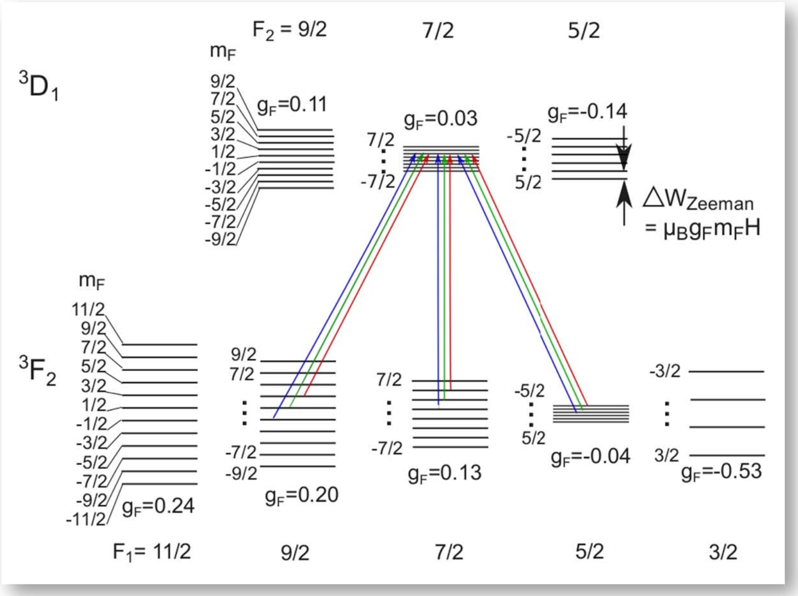

- Paschen–Back splitting (B >> 1 T)

  Transition splits 65-fold